Spatial and temporal analysis of changes in hydrological fluxes and their relation to deforestation in the Madeira River basin

Torres, Eliana; Maskey, Shreedhar; Corzo, Gerald; Uijlenhoet, Remko; Solomatine, Dimitri

DOI
10.1016/j.ejrh.2025.102680

Publication date
2025

Document Version
Final published version

Published in
Journal of Hydrology: Regional Studies

Journal of Hydrology: Regional Studies 61 (2025) 102680

Contents lists available at ScienceDirect

Journal of Hydrology: Regional Studies

journal homepage: www.elsevier.com/locate/ejrh

Spatial and temporal analysis of changes in hydrological fluxes and their relation to deforestation in the Madeira River basin

Eliana Torres [a,b,*], Shreedhar Maskey [c], Gerald Corzo [d], Remko Uijlenhoet [a], Dimitri Solomatine [a,b]

[a] Delft University of Technology, Department of Water Management, The Netherlands
[b] IHE Delft Institute for Water Education, Hydroinformatics and Socio-Technical Innovation, The Netherlands
[c] IHE Delft Institute for Water Education, Water Resources and Ecosystems, The Netherlands
[d] IHE Delft Institute for Water Education, Coastal & Urban Risk & Resilience, The Netherlands

ARTICLE INFO

Keywords:
Deforestation
Evaporation
Streamflow
Precipitation
Madeira River basin
Amazon

ABSTRACT

Study region: Madeira River basin, southwestern Amazonia
Study focus: This study investigates spatial and temporal changes in precipitation, evaporation, and streamflow, and their relationship with deforestation in the Madeira River basin, the largest Amazonian sub-basin. We applied Mann-Kendall trend analysis, change-point detection, and correlation analysis across multiple spatial scales, using satellite, reanalysis, and observed data from 1981 to 2015. These methods enabled us to detect long-term trends, identify shifts, and quantify the relationships between forest loss and hydrological changes
New hydrological insights for the region: The basin experienced an average deforestation rate of 2810 km^2 per year from 2001 to 2020, predominantly in the Brazilian portion. Between 1981 and 2016, we observed statistically significant negative trends in precipitation, evaporation, and streamflow, especially in the most deforested areas during the wet season. Correlation analysis (2001–2015) showed a statistically significant and positive relationship between forest area and evaporation in wet months ($r = 0.73$, $p < 0.1$) and a negative correlation between forest area and streamflow during the same season ($r = –0.6$, $p < 0.1$). These findings highlight the critical role of forests in modulating hydrological processes, supporting the hypothesis that deforestation may reduce evaporation, alter moisture recycling, and slow the water cycle. While our results are robust, we acknowledge that factors such as climate variability and land management practices may also influence hydrological changes and should be considered in future research.

1. Introduction

The Amazon basin has experienced rapid land-use changes in recent decades, with deforestation being a critical concern for the scientific community. These changes, driven by agricultural expansion, infrastructure development, and other human activities, have been linked to alterations in precipitation, evaporation, and river discharge (Chagas et al., 2022; Dias et al., 2015; Fassoni-Andrade et al., 2021; Flores et al., 2024; Heerspink et al., 2020a; Paiva et al., 2023; Souza et al., 2020). The Madeira River basin, a major

* Correspondence to: Department of Water Management, Faculty of Civil Engineering and Geosciences, Delft University of Technology, Building 23, Stevinweg 1, 2628 CN, Delft, The Netherlands.
E-mail address: etorresperalta@tudelft.nl (E. Torres).

https://doi.org/10.1016/j.ejrh.2025.102680
Received 5 May 2025; Received in revised form 17 July 2025; Accepted 31 July 2025
Available online 8 August 2025

southern Amazon tributary spanning Bolivia (51 %), Brazil (42 %), and Peru (7 %), has been notably affected by high rates of deforestation, alterations in river discharge and severe floods and droughts (Gutierrez-Cori et al., 2021; Laureanti et al., 2024; Molina-Carpio et al., 2017; Papastefanou et al., 2022; Trancoso et al., 2009).This basin covers a diverse range of climatic zones,

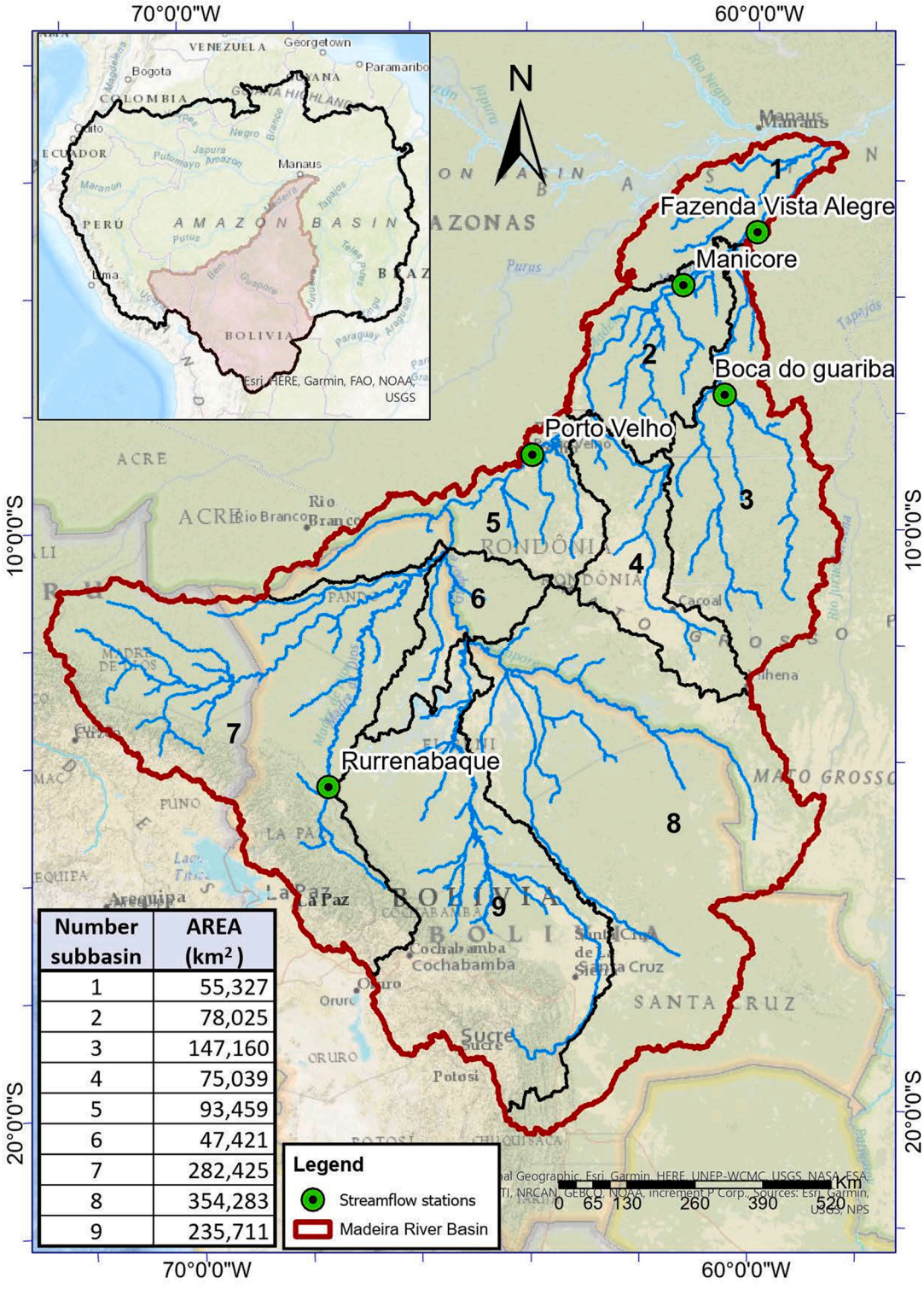

Fig. 1. Map of the Madeira River basin showing its nine subbasins (labeled by numbers for reference) and their respective areas (in km^2), major streamflow stations (green circles), and the basin's location within the Amazon basin (inset map).

extending from the Andean mountains to lowland rainforests. As a result, the interactions between deforestation and changes in hydrological processes are still poorly understood.

Research worldwide has demonstrated that land use change is a significant driver of hydrological processes at different timescales, influencing how local and regional basins respond to climate variability (Ayalew et al., 2024; Horton et al., 2021; Nguyen et al., 2023; Saraiva Okello et al., 2015; Slater et al., 2021). Previous studies have shown that urbanization can cause considerable increases and decreases in streamflow, including higher flood risk and lower base flows (Anderson et al., 2022; Blum et al., 2020; Hung et al., 2020; Oudin et al., 2018; Wu et al., 2015; Yang et al., 2021; Yang et al., 2016). The relationship between deforestation and changes in hydrological processes has also been reported globally. For example, studies in East Africa (Guzha et al., 2018), Malaysia (Abdulkareem et al., 2019), and Central America (Gotlieb and García Girón, 2020) have found that deforestation tends to decrease evapotranspiration and streamflow. In South America, however, research indicates that deforestation may lead to increase in streamflow (Posada-Marín and Salazar, 2022; Stickler et al., 2013; Weng et al., 2018).

In the Amazon basin, various studies have explored the impact of deforestation on hydrological variables (Cavalcante et al., 2019; Coe et al., 2009; Gutierrez-Cori et al., 2021; Heerspink et al., 2020; Lima et al., 2014; Staal et al., 2020). Some studies have reported that reduced forest cover diminishes evapotranspiration and alters precipitation patterns, leading to streamflow reduction in the southern Amazon (e.g., Heerspink et al., 2020; Marengo et al., 2018; Siqueira et al., 2015), while others have demonstrated that deforestation can increase river flow in the same region (Cavalcante et al., 2019; Levy et al., 2018; Lima et al., 2014). Posada-Marín and Salazar (2022) conducted a meta-analysis of different studies in the Amazon and concluded that the inclusion of deforestation effects precipitation both within and beyond basin boundaries often result in reduced rainfall and a subsequent decrease in river flow. They emphasized that the reduction in evaporation caused by deforestation can alter precipitation patterns across broader regions, leading to decreased discharge. These contrasting results highlight the complexity of hydrological responses to deforestation in the Amazon, which depend on factors such as basin size, timescale, and the influence of land-atmosphere interactions.

For the Madeira River basin in particular, researchers have documented trends in the hydroclimatic regime (Molina-Carpio et al., 2017; Sikora de Souza et al., 2020; Vergasta et al., 2023), and extensive forest loss (da Silva Cruz et al., 2022; de Souza et al., 2022a; Ferreira and Floreano, 2022; Flores et al., 2024; Gomes et al., 2022; Souza et al., 2020). However, the relation between spatial and temporal changes in precipitation, evaporation, and streamflow and deforestation in the basin remains poorly explored. Quantifying these effects is challenging due to the nonlinearity of runoff and evaporation dynamics, the difficulty of isolating deforestation impacts from climate variability, and the role of precipitation-evaporation feedbacks in modulating hydrological fluxes across multiple scales (Rogger et al., 2017).

This study aims to investigate the spatial and temporal changes in hydrological fluxes (precipitation, evaporation, and streamflow) in the Madeira River basin and assess their relationship with historical changes in forest cover. Our main hypothesis is that deforestation is associated with reductions in evaporation and alterations in precipitation-evaporation feedback and streamflow dynamics. To test this hypothesis, we apply non-parametric trend detection, change-point and correlation analyses using multi-source spatio-temporal datasets, including satellite-based land cover, precipitation and evaporation products, and observed streamflow data. This study provides a basin-wide perspective on the spatial co-occurrence of deforestation and hydrological changes across this transboundary region, and a subbasin-scale assessment of deforestation-related hydrological impacts in the Madeira River basin.

2. Data and methods

2.1. Study area

The Madeira River basin, located in the southwestern portion of the Amazon Basin, is the largest Amazonian sub-basin, with an area of 1368,850 km^2. It spans three countries: Bolivia (51 %), Brazil (42 %), and Peru (7 %) (Sikora de Souza et al., 2020). The Madeira is a

Table 1
Description and characteristics of the satellite, reanalysis, and observed data sources.

Variable	Source	Spatial/temporal resolution	Description
Land Cover Type	MODIS (Moderate Resolution Imaging Spectroradiometer)	500m/ Yearly (2001–2020)	Satellite data. MODIS/Terra+Aqua Land Cover Type, the MCD12Q1 Version 6.1 data product is derived using supervised classifications of MODIS Terra and Aqua reflectance data (Friedl and Sulla-Menashe, 2022)
Precipitation	CHIRPS v2.0 (Climate Hazards Group InfraRed Precipitation with Station)	0.25°/Daily (1981 – 2022)	Gridded rainfall time series based on satellite imagery with in-situ station data (Funk et al., 2015)
Evaporation	GLEAM 3.8a (Global Land Evaporation Amsterdam Model)	0.25°/ Daily (1980 – 2022)	The dataset is based on satellite and reanalysis data (MSWX net radiation and air temperature). It estimates the different components of land evaporation (often referred to as 'evapotranspiration') (Martens et al., 2017)
Streamflow	National Water and Sanitation Agency of Brazil (ANA) SO-HYBAM (Amazon basin water resources observation service) CAMELS-BR v1.1 (Catchment Attributes and Meteorology for Large-Sample Studies – Brazil)	Daily (1981–2016)	The observed data comes from five stream gauging stations, equipped with telemetric observation systems. These stations provide real-time data transmission and estimate streamflow by applying a stage-discharge relationship (rating curve) based on continuous river stage measurements

transboundary river with an estimated mean annual discharge of 31,200 m^3 /s at its confluence with the Amazon. The basin's mean annual rainfall is approximately 1834 mm/year with large spatial variability. Rainfall ranges from 255 mm/year at the Caracato station located at elevation 2650 m above mean sea level (masl) in the Bolivian Andes to over 3000 mm/year at stations located below 1500 masl (Molina-Carpio et al., 2017). Fig. 1 shows the Madeira river basin and its nine subbasins (labelled by numbers 1–9) derived from the HydroSHEDS data (spatial resolution 15 arc-second)(Lehner, 2014).

The wet season in the Madeira River basin typically occurs from December to May, with peak rainfall observed from January to March. The dry season is from June and November, with minimum rainfall during June to August. The basin has about two-month lag between the peak monthly basin average rainfall and peak monthly river discharge at the basin outlet, and therefore the maximum discharge is typically observed from March to May while the minimum discharge occurs from August to October (Espinoza Villar et al., 2009; Towner et al., 2020).

2.2. Data

2.2.1. Data sources and description

The data for this research were collected from different sources, including satellite/remote sensing-based, reanalysis and observed data depending on the type of data required and availability. These are described in Table 1.

The land-use land-cover maps for 20 years (2001–2020) were obtained from the version 6.1 Land Cover Type (MCD12Q1) of MODIS (Friedl and Sulla-Menashe, 2022). This product version is derived using supervised classifications of MODIS Terra and Aqua reflectance data. The dataset includes twelve different land cover types considering an annual classification of plant functional types (PFTs), which are categories used to classify vegetation based on their functional traits rather than their taxonomic classification.

The CHIRPS precipitation data was selected for this study due to its good performance in representing trends and patterns across the Amazon basin. Haghtalab et al. (2020) and Paca et al. (2020) cross-validated CHIRPS precipitation trends with data from local rain gauges, confirming its reliability. They reported correlation coefficients above 0.6, particularly in the lower part of the Madeira basin. Other studies have assessed CHIRPS by comparing it with different gridded datasets, such as Multi-Source Weighted-Ensemble Precipitation (MSWEP) and Tropical Rainfall Measuring Mission (TRMM), finding that CHIRPS trends consistently show the highest correlation with observed precipitation trends (with Spearman correlation coefficients of 0.62 for mean, and 0.61 for maximum, and 0.49 for minimum precipitation),and with the median value of the trends being similar to those observed at the weather stations (Chagas et al., 2022; De Souza et al., 2022b). Recently, CHIRPS data have been widely used in hydrological and environmental analyses within the Amazon basin, further supporting their reliability in reflecting interannual variability in the basin (Baker et al., 2021; Heerspink et al., 2020; Paredes-Trejo et al., 2021)

We used the GLEAM dataset due to its robust representation of actual evaporation. GLEAM combines satellite data with a hydrological model to provide accurate estimates of evaporation, accounting for various water sources such as soil moisture, vegetation, and interception loss (Martens et al., 2017; Miralles et al., 2011). This dataset has been validated in diverse ecosystems globally, where it has shown a strong correlation with flux tower measurements, typically with correlation coefficients ranging between $r = 0.78$ and 0.81 (Martens et al., 2017), making it particularly reliable for capturing seasonal and interannual evaporation variations (Miralles et al., 2016; Paca et al., 2019). Furthermore, this evaporation dataset has demonstrated to be valuable for Amazon basin studies due to its high spatial and temporal resolution, and its ability to separate evaporation into components (e.g., soil evaporation, transpiration, canopy interception) (Chagas et al., 2022; Gomes et al., 2022). These characteristics make GLEAM particularly useful for analysing the hydrological impacts of deforestation in this region.

2.2.2. Data pre-processing

Since the detailed classification provided by MODIS plant functional types was not essential for the scope of this study, land cover types were simplified into eight broader categories: Water, Forest, Shrub, Grass, Cropland, Urban, Snow and Ice, and Non-Vegetated Lands. This grouping was conducted using ArcGIS version 10.8 geoprocessing tools, focusing on general land cover types relevant to deforestation and hydrological analysis. The simplified categories represent the primary land use and vegetation patterns in the study

Table 2
Land cover types, including the classification of PFTs from MODIS and the grouped classes.

MODIS land cover types (LC_Type5)	Grouped Land-cover type	Description
Water Bodies	Water	At least 60 % of area is covered by permanent water bodies.
Evergreen Needleleaf Trees Evergreen Broadleaf Trees Deciduous Needleleaf Trees Deciduous Broadleaf Trees	Forest	Dominated by evergreen conifer, broadleaf, palmate and deciduous trees (>2 m). Tree cover > 10 %.
Shrub	Shrub	Shrub (1-2m) cover > 10 %.
Grass	Grass	Dominated by herbaceous annuals (<2 m) that are not cultivated.
Cereal Croplands Broadleaf Croplands	Cropland	Dominated by herbaceous annuals (<2 m), including cereal croplands and broadleaf croplands.
Urban and Built-up Lands	Urban	At least 30 % impervious surface area including building materials, asphalt, and vehicles.
Permanent Snow and Ice	Snow and Ice	At least 60 % of area is covered by snow and ice for at least 10 months of the year.
Non-Vegetated Lands	Non-Vegetated Lands	At least 60 % of area is non-vegetated barren (sand, rock, soil) with less than 10 % vegetation.

area. The original PFTs categories and the grouped version used in this study are shown in Table 2.

The hydrometeorological data were pre-processed to ensure high data quality and minimal gaps. The precipitation and evaporation data from the CHIRPS and GLEAM datasets were nearly continuous, requiring no additional gap-filling for this analysis. Additionally, due to the reliability of these products and their extensive quality control prior to release, it was not necessary to apply additional filtering or pre-processing to these datasets. The pre-processing of the daily streamflow data consisted of removing the stations with more than 5 % of missing values, selecting just 5 stations (Fig. 1). The ANA applies rigorous quality-control procedures to its streamflow monitoring network, including instrument calibration, rating-curve updates, periodic maintenance, and consistency checks, as well as homogeneity and stationarity testing, and trend/jump detection in the time series (ANA, 2011). Given the quality assurance already performed by ANA and our criterion for the missing values, no further outlier removal was considered necessary.

To assess the consistency of the hydrometeorological data, we performed a basic water balance check by comparing the annual difference between precipitation and evaporation ($P - E$) with annual observed discharge. Closing the water balance in a complex system like the Amazon basin is challenging due to the intricate feedback processes between evaporation and precipitation, which involve significant spatial and temporal variability (Marengo, 2005). Despite these complexities, this approach is useful for assessing the reliability of datasets, especially in analyzing long-term trends and correlations. Paca et al. (2019) and Cavalcante et al. (2019) have demonstrated the effectiveness of this approach in verifying the quality and applicability of datasets for hydrological assessments in tropical ecosystems. We found a difference of 17–32 % between the GLEAM reanalysis dataset and catchment-derived evaporation (E) values evaluated at three discharge gauges (Porto Velho, Manicoré, and Fazenda Vista Alegre). While this uncertainty falls within expected limits for large-scale hydrological analysis, it highlights the importance of considering these uncertainties when interpretating the results.

2.3. Methods

The methodological approach of this study consisted of three main analytical components: (i) land cover change analysis, (ii) trend and change point detection, and (iii) correlation analysis.

2.3.1. Land cover change analysis

We estimated land-use and land-cover (LULC) changes across the Madeira River Basin and at regional and subbasin scales using MODIS multitemporal Landsat imagery with a 500 m spatial resolution over a 20-year period (2001–2020). To achieve this, LULC maps were first delineated by basin boundaries and then subdivided by country and subbasin delineations. Using ArcGIS 10.8.1 geoprocessing tools, we calculated the annual area (km^2) of each land cover type and quantified transitions between LULC categories.

We then calculated the net forest change for the full 20-year study period, as well as the annual, 5-year, and 10-year rates of change in forest area to capture both short- and long-term dynamics. Net forest change reflects the cumulative forest area change, balancing gains and losses over the study period. Additionally, we used land cover conversion data to calculate the gross forest loss at basin, regional, and subbasin scales, which quantifies total deforestation by indicating the extent of forest converted to other land uses, excluding afforestation. This dual analysis, recently used by Estoque et al. (2022) provides comprehensive information about historical deforestation patterns across multiple spatial and temporal scales.

2.3.2. Trend and change point detection

To identify significant trend in the historical series of forest cover and hydrological fluxes, we used the *mannkendall* function from the *scipy.stats* library in Python to apply the nonparametric Mann-Kendall test for trend detection (Kendall, 1975; Mann, 1945), setting a significance level of $\alpha = 0.1$. The test was applied to the data series considering two different spatial scales: the subbasin scale for the forest cover, precipitation, evaporation, and discharge data, and the 0.25° grid scale for forest cover, precipitation, and evaporation. Different temporal scales were also considered for this analysis: annual for forest cover, and annual, seasonal, and monthly for precipitation, evaporation and discharge. For the subbasin-scale analysis, areal average daily timeseries were obtained from the grid-based daily timeseries of precipitation and evaporation per subbasin. These timeseries were then aggregated to compute monthly, seasonal and annual values. The Mann-Kendall test has been widely applied and is considered the most suitable for non-normally distributed data, which is often the case for hydrometeorological variables (e.g., de Souza et al., 2022a; Heerspink et al., 2020; Min, 2006; Tsiokanos et al., 2024; Yue et al., 2002). In the pixel-based analysis, we used the Kendall's Tau coefficient (τ), to quantify the strength and direction of trends. Positive τ values indicate increasing trends, while negative values represent decreasing trends, with the magnitude reflecting the strength of the trend (Kendall, 1975). Before performing the trend analysis, the serial correlation (or persistence) of the timeseries was evaluated. When was necessary, the autocorrelation was reduced by pre-whitening the data to ensure the validity of the subsequent test (Helsel and Hirsch, 2002; Min, 2006; Yue et al., 2002).

If a trend was detected, we estimated the magnitude of the trend (slope) using the Theil-Sen slope estimator (Sen, 1968; Theil, 1950). This robust nonparametric method is less sensitive to outliers and computes the slope by taking the median of slopes between all possible pairs of data points (Helsel and Hirsch, 2002). This ensures that the estimated slope reflects the central tendency of the data, even when extreme values are present. The slope was calculated for annual data series of the forest cover, precipitation, evaporation and discharge, and for seasonal and monthly precipitation, evaporation and discharge.

We applied The Pettitt test (Pettitt, 1979) to identify any abrupt changes in the annual data series on each subbasin. This test evaluates the probability of a change point at each time step in the series by comparing the distribution of data values before and after each potential change point. Once a significant change point was identified, the time series was divided into two subsets: one before and one after the change point. A two-sided t-test at a significance level of 0.1 was then applied to evaluate the difference between the

means of the two subsets, and to assess the impact of the change on the monthly regime of precipitation, evaporation and discharge.

2.3.3. Correlation analysis

Finally, we applied the Spearman rank correlation to analyse the relationship between annual and monthly time series of precipitation, evaporation, and discharge, and the annual forest coverage. The correlation calculations were performed using the *spearmanr* function from Python's *scipy.stats* library, which provides both the Spearman rank correlation coefficient (*r*) and its associated *p-value.* The level of association between the mentioned variables was evaluated through both the correlation of the raw time series and the correlation of changes in the time series. The Spearman rank correlation coefficient, *r*, measures the strength and direction of the monotonic relationship between two variables, that is, when one variable consistently increases or decreases as the other increases. This coefficient is resistant to outliers, which is an important feature for application in water resources (Helsel and Hirsch, 2002). Despite both Spearman and Kendall's Tau being used to measure monotonic correlation, we opted for Spearman's correlation due to its robustness in the presence of tied values, which are common in hydrological data (Yue et al., 2002). Given the temporal availability of all datasets, the correlation analysis was conducted over a 15-year period, from January 2001 to December 2015, with statistical significance tested at the $\alpha = 0.1$ level. Although $\alpha = 0.05$ is generally a more preferred significance level used in hypothesis testing, 0.1 is also commonly used in hydrological trend analysis (e.g. Conte et al., 2019; Haghtalab et al., 2020; Heerspink et al., 2020; Hu et al., 2012). Helsel and Hirsch (2002) and Helsel et al. (2020) also suggested a more flexible threshold value, e.g. 0.05 or 0.01. The main reason for allowing a higher threshold value (e.g. 0.1 instead of 0.05) is to reduce the risk of Type II errors (i.e., failing to detect a trend that may be present), particularly in a data-scarce situation commonly encountered in the large basin or regional scale

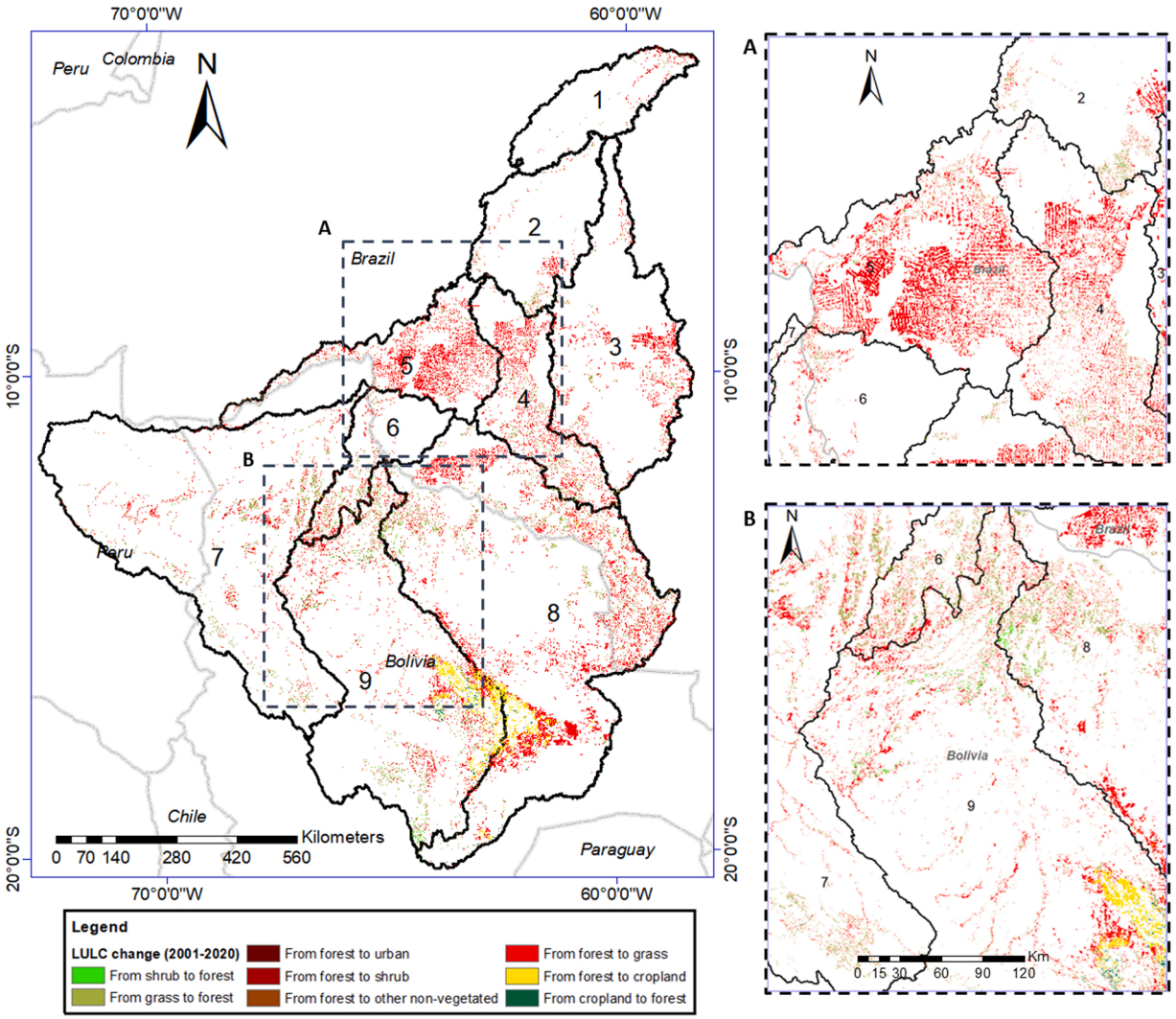

Fig. 2. Changes in land use for the period of 2001–2020 in the Madeira River basin and its subbasins (Subbasins labelled by numbers) A. Zone mostly dominated by deforestation (conversion from forest to grass). B. Zone with different types of changes, including also afforestation (from cropland and shrub to forest).

hydrological analysis.

3. Results

3.1. Land use change

The analysis of the multitemporal Landsat images during the 20-year period (2001–2020) shows significant changes in the land-use and land-cover across the entire Madeira River basin. The conversion from forest to other land-use classes such as grass and cropland were the most pronounced changes (See Fig. 2). During the study period, grassland area increased by 45,629 km^2 (3.33 % of the basin area), while forest area decreased by 53,471 km^2 (3.91 %), representing the net forest change. This corresponds to a deforestation rate of 2670 km^2 per year (0.20 %) from 2001 to 2020, with the highest rate of change between 2015 and 2020 of 6, 214 km^2 per year (0.45 %). A detailed 5-year, and 10-year rates of change are presented in supplementary material, Figure S1 and S2.

The regional analysis shows different land use change dynamics in the three countries that share this transboundary basin. For instance, in the Brazilian and Peruvian parts of the basin, the dominant conversion is from forest to grassland (Fig. 4A). In the Bolivian part, however, land cover is also converted from forest to cropland, as well as from grassland and shrub to forest (Fig. 4B). Deforestation patterns also differ among countries based on land-use policies: In Brazil, deforestation mostly follows spatially linear patterns, with clear-cutting along roads and property boundaries. These structured patterns are commonly attributed to the expansion of large-scale cattle ranching and associated infrastructure (Coe et al., 2009; Lima et al., 2014; Souza et al., 2020). In contrast, deforestation in Bolivia appears less structured and more dispersed, likely influenced by smaller-scale farming and a mixture of land uses (Müller et al., 2014).

The Sankey diagram (Fig. 3), presents the land cover change dynamics within the study period. Although Bolivia comprises the majority of the Madeira River basin (51 %), the area of forest conversion is larger in Brazil, with a gross loss of 37,380 km^2, of which 98 % was converted to grassland. In Bolivia, the gross forest loss is 35,172 km^2, with 75 % converted to grassland and 22 % to cropland. These findings indicate that the Brazilian portion of the basin is the most altered and significantly affected by deforestation, which supports and complements the results of previous research on deforestation in the Amazon and in each of the three countries (da Silva Cruz et al., 2022; Flores et al., 2024; Siqueira et al., 2015)

The subbasin level analysis reveals that subbasins 5 and 4 have the highest percentages of gross forest loss over the 20-year study period, with 12.2 % and 9.4 %, respectively. In contrast, subbasin 2 has the lowest forest loss percentage at 1.5 % (see Fig. 4). Across most subbasins, forest is primarily converted to grassland, while in subbasins 8 and 9 conversion from forest to cropland is also notable.

Additionally, Fig. 5 presents the temporal trend analysis of the annual net forest change per subbasin (including losses and gains),

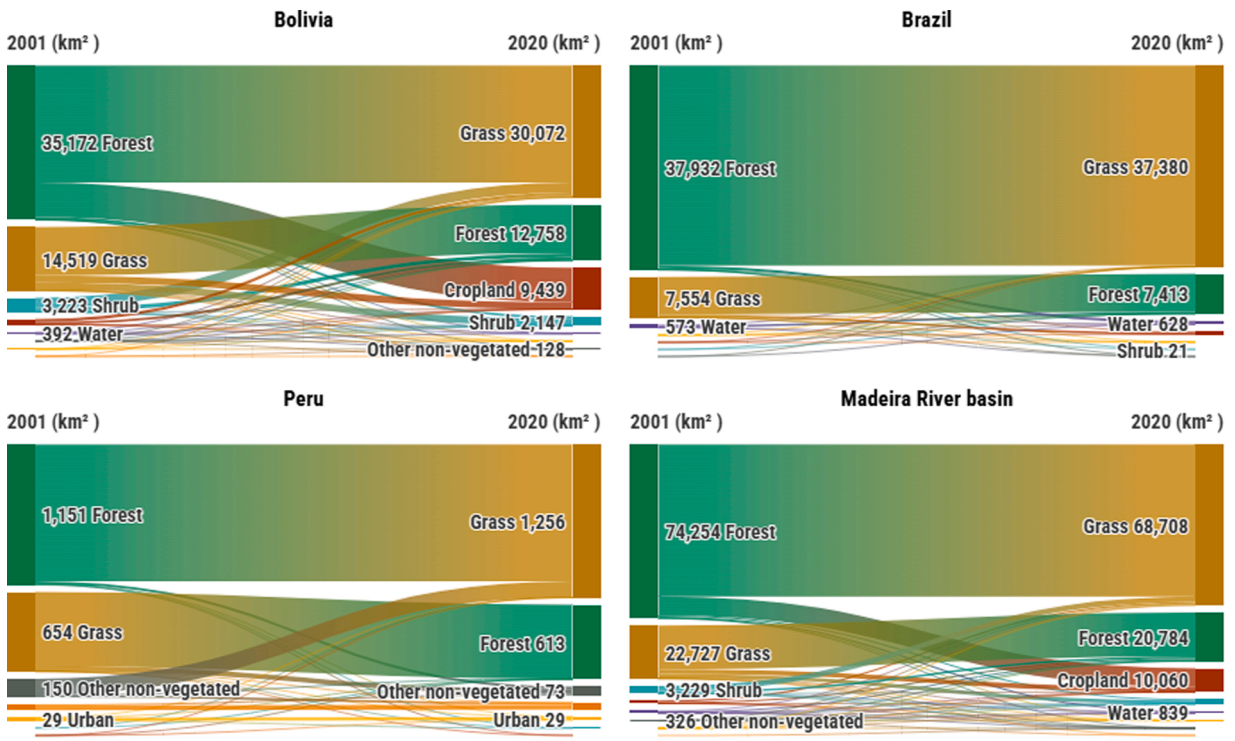

Fig. 3. Land cover change dynamics within the Bolivian, Brazilian, and Peruvian portions of the Madeira River basin, as well as across the entire basin. Only areas that underwent a land cover conversion (e.g., forest to grassland or cropland) are included, while stable land cover types (e.g., forest remaining as forest) are omitted for visual clarity. Diagram generated using Flourish data visualization tool.

showing a significant decreasing trend in forest coverage across all subbasins (at a significance level of 0.1). Notably, subbasins 5 and 4 exhibit the steepest slopes in the deforestation trend. This indicates an average forest coverage reduction of 4.6 % per decade in subbasin 5 and −2.6 % over the same period in subbasin 4. Subbasin 8, the largest subbasin, shows a negative trend of forest change with 9184 km^2 of forecast area reduction in 10 years on average. Subbasin 7, a transboundary subbasin between Bolivia and Peru, exhibited a period of afforestation from 2007 to 2011, followed by deforestation from 2010 to 2019. As a result, the rate of forest cover change in the entire period in subbasin 7 is slightly negative.

3.2. Changes in hydrological fluxes at subbasin-scale

3.2.1. Evaporation

Fig. 6 summarizes the results of the trend analysis for annual evaporation. The trend slope for each subbasin is presented, alongside the results of the change point analysis for subbasins 1, 4, 6, and 9. These subbasins were the only ones that exhibited a significant change point (at a significance level of 0.1) in their time series data. Thus, their average monthly evaporation regime before and after the year of change is also shown in the figure.

The results of the Mann-Kendall test reveal significant trends at α= 0.1 for subbasins 1 and 7 during the period 1980–2022, with evaporation increasing by 1.58 mm/year and 0.94 mm/year, respectively. These increasing trends in the monthly evaporation regime are predominantly observed during the dry months, as seen in subbasins 1, 7, 6 (Figs. 6A), and 9 (Fig. 6B). Although the trends for subbasins 2, 4, and 8 are not statistically significant at α= 0.1, their annual evaporation shows a decreasing pattern. Subbasin 4 demonstrates the strongest negative trend slope, with evaporation declining by 0.69 mm/year. The comparison of the monthly regimes for the periods 1980–2002 and 2003–2022 (Fig. 6D) indicates that the reduction in evaporation in subbasin 4 is mostly during the wet season, with a decrease of up to 7.8 % in February.

The trend slopes of the average monthly evaporation per subbasin for the period of 1981–2022 are presented in Fig. 7. The results reveal distinct spatial and temporal variation in the monthly evaporation trends. The spatial variation (i.e., between subbasins) is most pronounced during the dry season, particularly in September. During this month, half of the basin exhibited increasing trend in monthly evaporation (subbasins 1, 5, 6, 7, and 9), while the other half showed a decreasing trend (subbasins 2, 3, 4, and 8). In contrast, during the wet season, the evaporation trends presented a more uniform spatial pattern. Most subbasins displayed a significant decreasing trend in monthly evaporation at α= 0.1, with the exception of subbasin 7, which showed a significant increasing trend.

Confirming the results of the change point analysis, we found that the monthly evaporation in subbasin 7 shows an increasing trend for all the months, with the steepest trend for September (dry season) at 0.49 mm /year. Subbasin 8 exhibits the most pronounced negative trend, with a slope of −0.37 mm/year in September, while the steepest significant decreasing trend for subbasin 4 (-0.33 mm/year) was observed in February (wet season). These findings confirm that although the annual evaporation trends are not statistically significant in most of the subbasins, half of the Madeira subbasins are showing a significant decreasing trend in monthly evaporation, mostly in the wet season. The detailed trend slopes for yearly and monthly evaporation, and the spatial distribution of seasonal evaporation trends are presented in the supplementary material, Table S1, and Figure S3 respectively.

3.2.2. Precipitation and discharge

The results of the trend analysis for annual precipitation and discharge (1981–2016) are shown in Fig. 8, including also the results

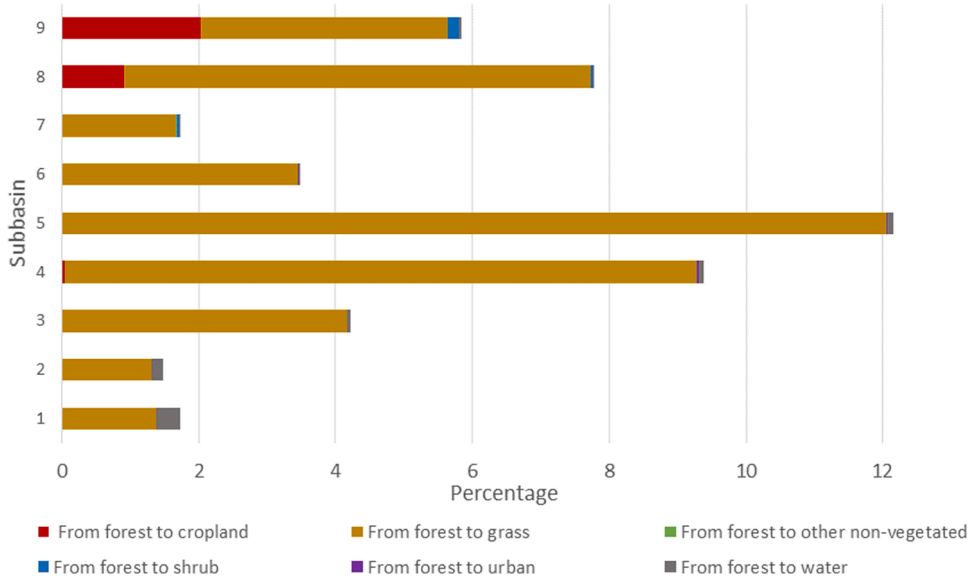

Fig. 4. Percentage of gross forest loss per subbasin over the 20-year study period, showing primary land cover transitions in each subbasin.

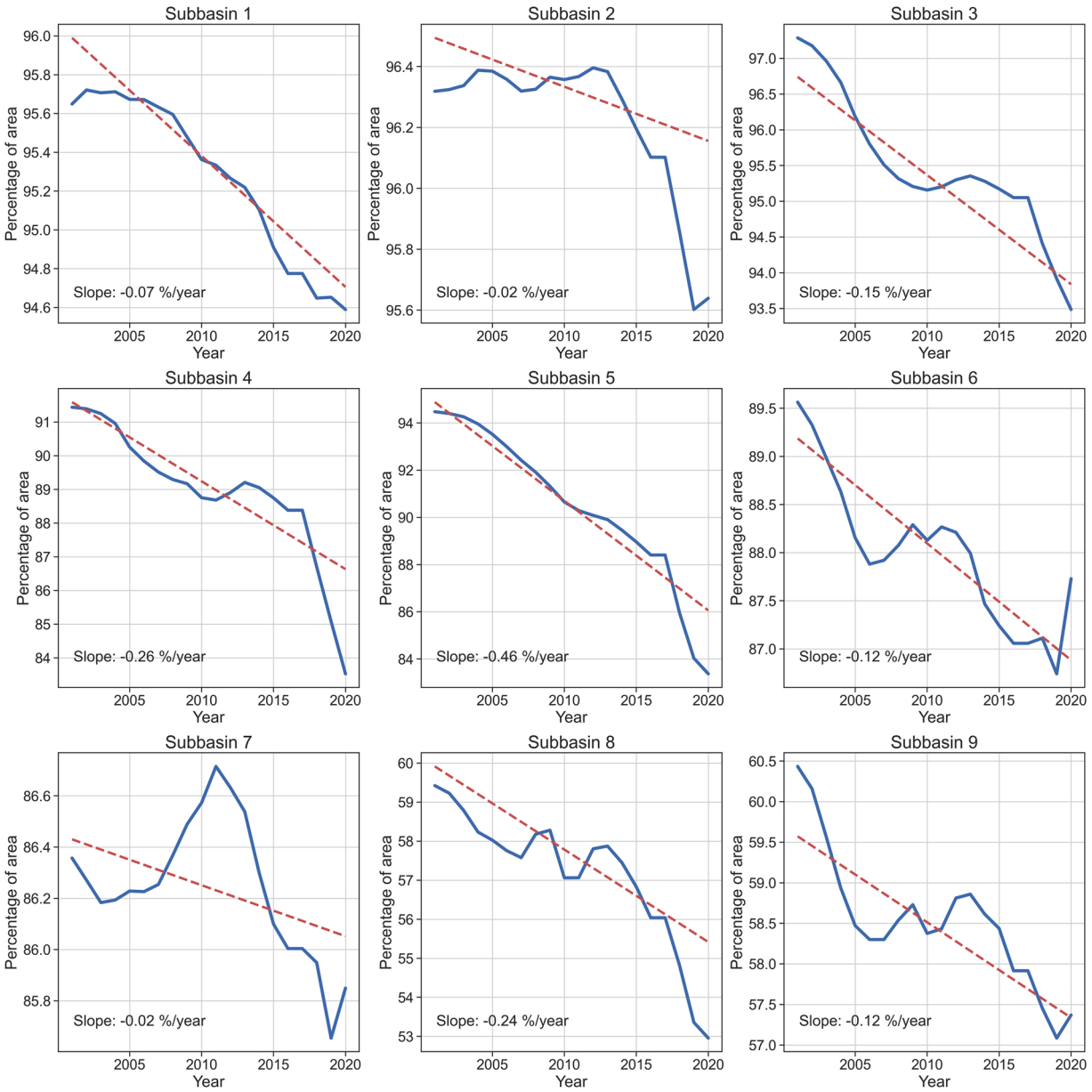

Fig. 5. Deforestation trend over time per subbasin. The solid line represents annual deforestation data as a percentage of total area, while the dashed line indicates the fitted trendline using the Theil-Sen estimator. The calculated slope reflects the rate of deforestation change per year. All subbasins present a p-value less than 0.1 from the Mann-Kendall test, indicating the statistical significance of the trend. To highlight changes within each subbasin, y-axes are scaled individually. For inter-subbasin comparison, see Fig. S3 of the supplementary material, which shows standardized slopes.

for the change point analysis for the stations Fazenda Vista Alegre and Manicore, located downstream of subbasins 2. These stations exhibit a significant change point in the discharge regime in 1996. We found that subbasins 2 and 4 are the most affected with statistically significant decrease in precipitation: slope −8.3 and −3.1 mm/year, respectively. The highest negative trend in discharge was found for station Manicore, with a reduction of 4.5 mm/year. This station also shows the most notable change in the monthly regime, with around 34 % less discharge in October (dry season) in the post-change point period (1996–2016) than in the pre-change point period (1981–1995) (Fig. 8D). These findings are consistent with results from previous studies conducted in the Amazon basin, for instance, Heerspink et al. (2020) showed a decreasing dry season precipitation in the upper Madeira Basin.

The subbasin-scale trend analysis on monthly precipitation and discharge indicate that changes in precipitation are less spatially variable compared to the trends in evaporation (See Fig. 9). Nevertheless, precipitation is found to be decreasing in most subbasins, with the most pronounced reductions occurring from November to January (wet season). In these months, subbasins 2, 8, and 9

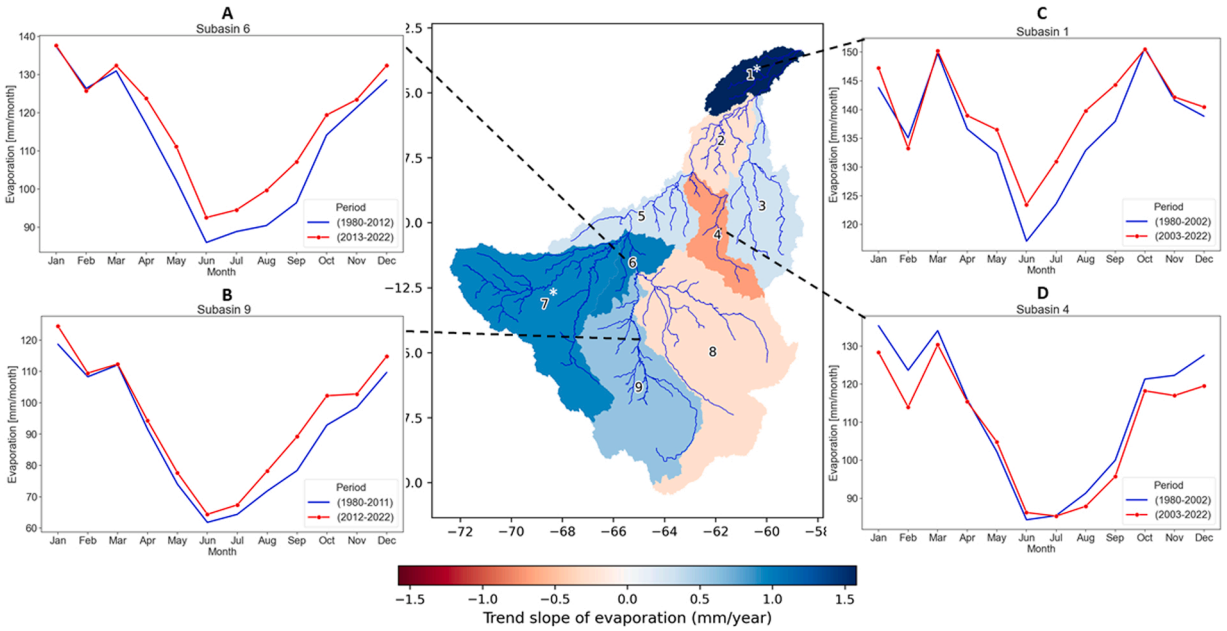

Fig. 6. Trend slopes (mm/year) for total annual evaporation across the subbasins of the Madeira River Basin during the period 1981–2022, with asterisks marking statistically significant trends at the α= 0.1 level. The monthly evaporation regimes for subbasins with detected change points are also shown: subbasin 6 (A), subbasin 9 (B), subbasin 1 (C), and subbasin 4 (D).

showed a statistically significant downward trend, with a maximum slope of up to −1.8 mm/year in January for Subbasin 8. During the dry season, particularly in September, there is a decreasing trend in precipitation across the entire Madeira River basin, with the most significant reductions observed in subbasins 1, 2, and 3. In contrast, and confirming the findings for annual precipitation, Subbasin 7 (which spans from north-western Bolivia to north-eastern Peru) exhibited higher temporal variability. This subbasin showed a significant increasing trend in December and February (the wettest months), which may offset the decreasing trends observed in the other months.

Overall, the discharge shows a decreasing trend in most months and at downstream stations, with the highest negative trends in May and June (dry season). The highest negative trend slopes were observed at the Manicore station, with significant discharge reductions ranging from 0.30 to 0.72 mm/year (151–176 m^3/s) from June to December. This station is located downstream, where it collects all the water from the middle and upper parts of the basin. Therefore, the trend at this point provides critical information about the streamflow changes and their impacts on the entire basin, highlighting a greater potential impact during the dry season. On the other hand, the station Rurrenabaque, located in the Andean region of the basin (subbasin 7) showed statistically not significant trends in most months, indicating that discharge in this area did not experience substantial changes during the study period. This aligns with Molina-Carpio et al. (2017) in their analysis of the upper part of the basin, where they found a decreasing trend in baseflow in the lowland tributaries, but no significant trend in the Andean tributaries.

Generally, the trend analysis of the hydrological fluxes indicates that precipitation, evaporation, and streamflow are all changing in the Madeira River Basin during the period considered in our analysis, with statistically significant negative trends observed during wet season for evaporation and during dry season for discharge. The Andean region of the basin (subbasin 7) is the least affected in terms of changes in these three hydrological fluxes, while Subbasins 2, 4 and 8, located in the middle part of the basin, show the highest impact, primarily through decreasing trends in precipitation and evaporation. These reduced precipitation in these subbasins likely contributed to the significant decrease in downstream discharge observed at the Manicore station.

3.3. *Changes in hydrological fluxes at pixel-scale*

The pixel-based trend analysis reveals important similarities between the areas of hydrological flux variations and the loss of forest coverage across the Madeira River basin (See Fig. 10). The results are presented in terms of the Kendall τ coefficient, which indicates the strength and direction of the trends. Although the computed τ values are low ($<= |0.4|$), the results provide important information to identify areas experiencing increases or decreases in evaporation and precipitation. For example, the areas with the strongest negative trends in evaporation, such as subbasins 4, 5, and 8, align with regions of significant deforestation (Fig. 10A). Although these results may indicate that changes in evaporation coincide with areas of deforestation, this correspondence does not necessarily imply direct causation. However, it highlights the regions with deforestation and evaporation changes that may require attention and future attribution studies when more/improved data become available.

In addition, the precipitation trends show weaker τ values compare to evaporation, reflecting the challenge of establishing a direct,

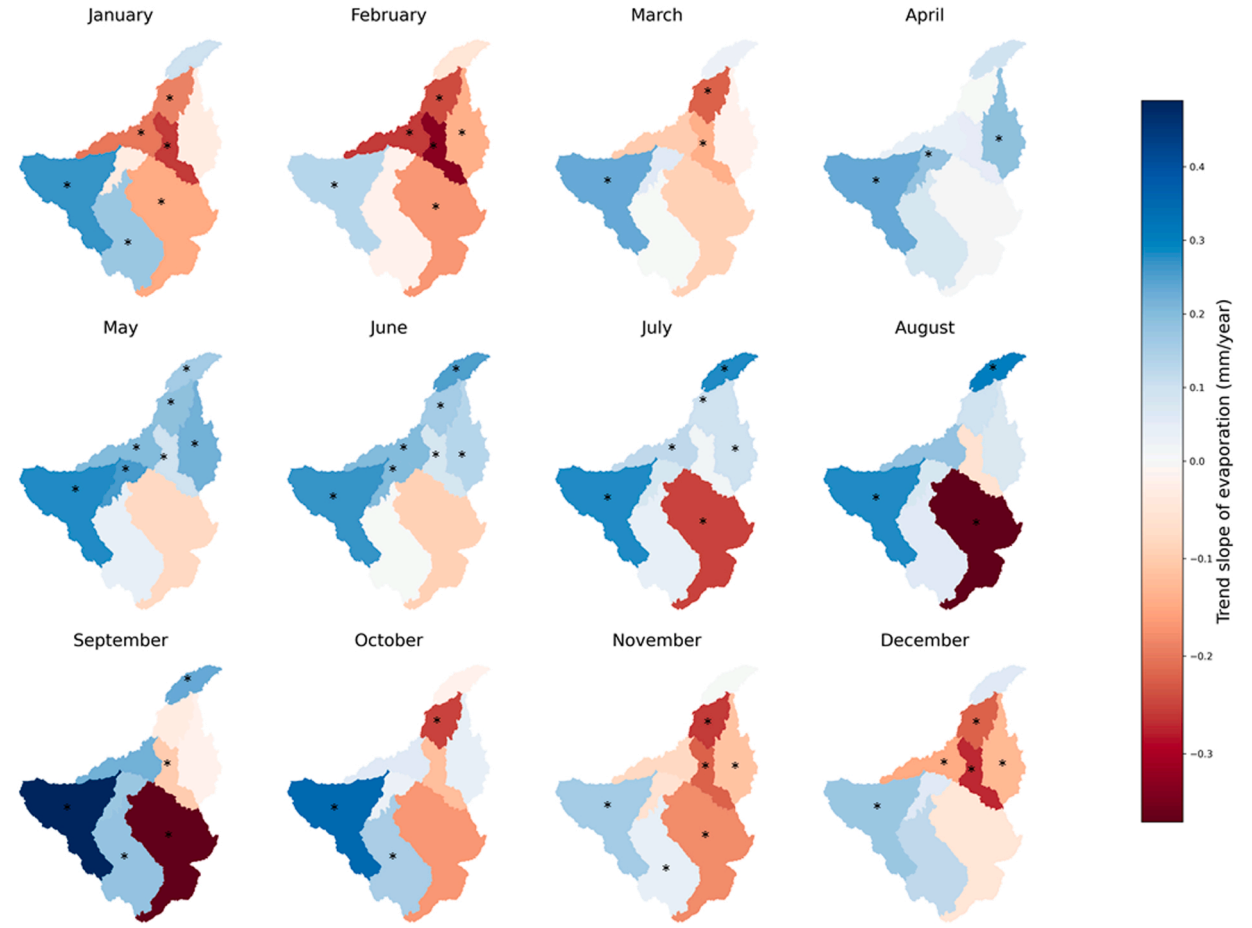

Fig. 7. Monthly trends of evaporation (mm/year) in the Madeira River Basin (1981–2022). Blue shades represent positive trends, indicating increasing evaporation, while red shades represent negative trends, indicating decreasing evaporation. The asterisks (*) mark subbasins where the trends are statistically significant at the 0.1 level. Notable trends include strong positive slopes during wet months (August and October) in the southern subbasins and negative slopes during wet season in the center and northern subbasins.

site-specific correlation between deforestation and local precipitation changes. The complexity of land-atmosphere interactions in the Amazon and the spatial and temporal variability of moisture recycling processes further complicates this relationship (Nobre et al., 2021). As Eltahir (1996) explains, the recycling ratio (the proportion of precipitation derived from local evaporation) varies with scale, being nearly zero for small areas but higher for large regions like the Amazon basin. Moreover, studies like Van Der Ent et al. (2010) and Zemp et al. (2014) reveal spatial variation within the basin, with recycling ratios near zero at the river's mouth and over 50 % near the Andes due to topographic effects that increase precipitation and limit moisture outflow.

3.4. Analysis of correlations between hydrological fluxes and forest area

Based on Spearman's rank coefficients between annual evaporation and forest cover (see Table 3), statistically significant and moderate positive correlations are observed in Subbasins 3 ($r = 0.50$) and 5 ($r = 0.46$). These values suggest that the reductions in forest areas may be linked to the decreases in evaporation rates in these subbasins. Although the correlation in the neighbouring Subbasin 4 does not reach the statistical significance level 0.1 ($p = 0.12$), it also presents a moderate positive correlation ($r = 0.42$). Conversely, subbasin 6 shows a statistically significant negative correlation ($r = -0.63$, $p < 0.1$) even though deforestation is also observed in this subbasin. However, since subbasin 6 is not experiencing high rates of deforestation (0.15 %/year, compared to 0.46 %/year in subbasin 5) and is located closer to the Andean region (characterized by higher water recycling ratios and influenced by regional precipitation dynamics) its evaporation patterns may be shaped more by atmospheric and climatic mechanisms than by land use changes.

The monthly correlation analysis (see Fig. 11) shows notable seasonal dynamics. Positive correlations between forest cover and evaporation are most pronounced in Subbasins 3, 4, and 5 during the wet season (January–February) and during the transition to the dry season (October–November). In contrast, Subbasins 1 and 6 exhibit negative correlations during the dry season (June–August). This seasonal variation in the correlations suggests that evaporation may be more sensitive to forest cover changes during wet periods.

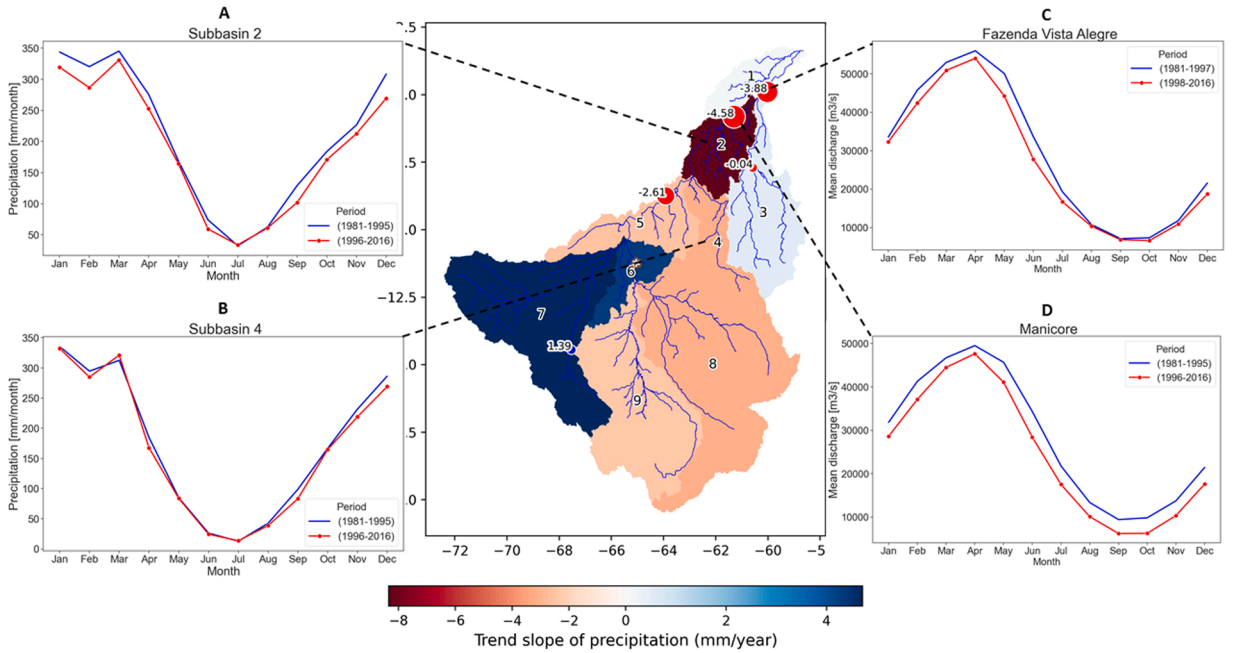

Fig. 8. Trends in precipitation and discharge in the Madeira River Basin. The central map illustrates the trend slope of precipitation (in mm/year) across subbasins (labelled by numbers), with a colour gradient indicating positive (blue) and negative (red) trends. Panels A and B show the mean monthly precipitation in Subbasins 2 and 4, respectively, comparing two periods: pre- and post-impact periods identified through the Pettitt test (1981–1995 and 1996–2016). Panels C and D display the mean monthly discharge at two monitoring stations, Fazenda Vista Alegre and Manicore, where change points were detected, highlighting similar pre- and post-impact periods.

For example, Subbasins 4 and 5, which show higher deforestation trends (-0.30 and −0.53, respectively), have positive correlations with evaporation during the wet season, as reflected in the decreasing evaporation trends (Figs. 6 and 7). Conversely, Subbasins 1 and 6, with lower deforestation trends (-0.07 and −0.11, respectively), exhibit inverse correlations during the dry season, consistent with their non-significant (but increasing) trend in evaporation.

The correlation analysis between forest area and annual discharge reveals varying degrees of negative association across different stations within the Madeira River basin (See Table 4). At the Porto Velho station, which collects runoff from subbasins 5, 6, 7, 8, and 9, a statistically significant correlation coefficient of $r = -0.46$ was observed. This suggests a moderate inverse relationship, where decreases in forest area are associated with increases in annual discharge. The significant positive correlation between changes in forest and changes in discharge ($r = 0.48$) further supports the notion that alterations in discharge may be related to forest cover changes. Moving downstream, the strength of this negative correlation diminishes, with the Manicore station (that also includes subbasin 2, 3, and 4), exhibiting a correlation coefficient of $r = -0.21$. This weaker and non-significant inverse relationship could reflect the large basin area and the heterogeneity of land use dynamics in the middle and upper parts of the basin. These results highlight the challenges in establishing a clear relationship between land use and hydrological responses at larger scales.

The monthly correlation analysis (see Fig. 12) reveals that the highest correlation coefficients are observed during the wet months of the discharge regime (February to May) at Porto Velho and Manicore stations, and from June to August at Fazenda Vista Alegre station (near the basin outlet). Specifically, the highest value was found in May for the Porto Velho station ($r = -0.6$, $p < 0.1$), indicating a moderate to strong inverse relationship between forest cover and discharge. These results suggest that in this part of the basin streamflow of April and May is more sensitive to changes in forest cover, which may be related to the two-month lag following the peak rainfall in March. Thus, with less forest cover, hydrological processes in the basin such as infiltration and soil moisture may be reduced, leading to increased discharge.

Additionally, our results of the analysis of the seasonal cycle suggest a shift in the timing of yearly peak precipitation in recent years, which could amplify these hydrological sensitivities. For instance, in Subbasins 3, 4, and 5, the precipitation peak shifted from December and January (2004–2013) to March (2014–2022). This aligns with the findings by Nobre et al. (2021), which reported a lengthening of the dry season in regions experiencing deforestation at moderate to large scales (10–1000 km^2). Such shifts in precipitation timing, coupled with reduced forest cover, are likely to influence the basin's hydrological balance further, altering the regional hydrological cycle.

Among all the variables evaluated, the most relevant results were found in the correlations between forest area and evaporation (evaluated per subbasin), and between forest area and discharge (calculated at three streamflow stations primarily located lower part of the basin; see Supplementary Figure S5 for monthly correlations between all variables at each station). Using CHIRPS, GLEAM, and observed datasets, our findings confirm the significant influence of forest cover on hydrological processes. The use of GLEAM dataset, which captures the tall canopy vegetation component and distinguishes between different vegetation types (Martens et al., 2017),

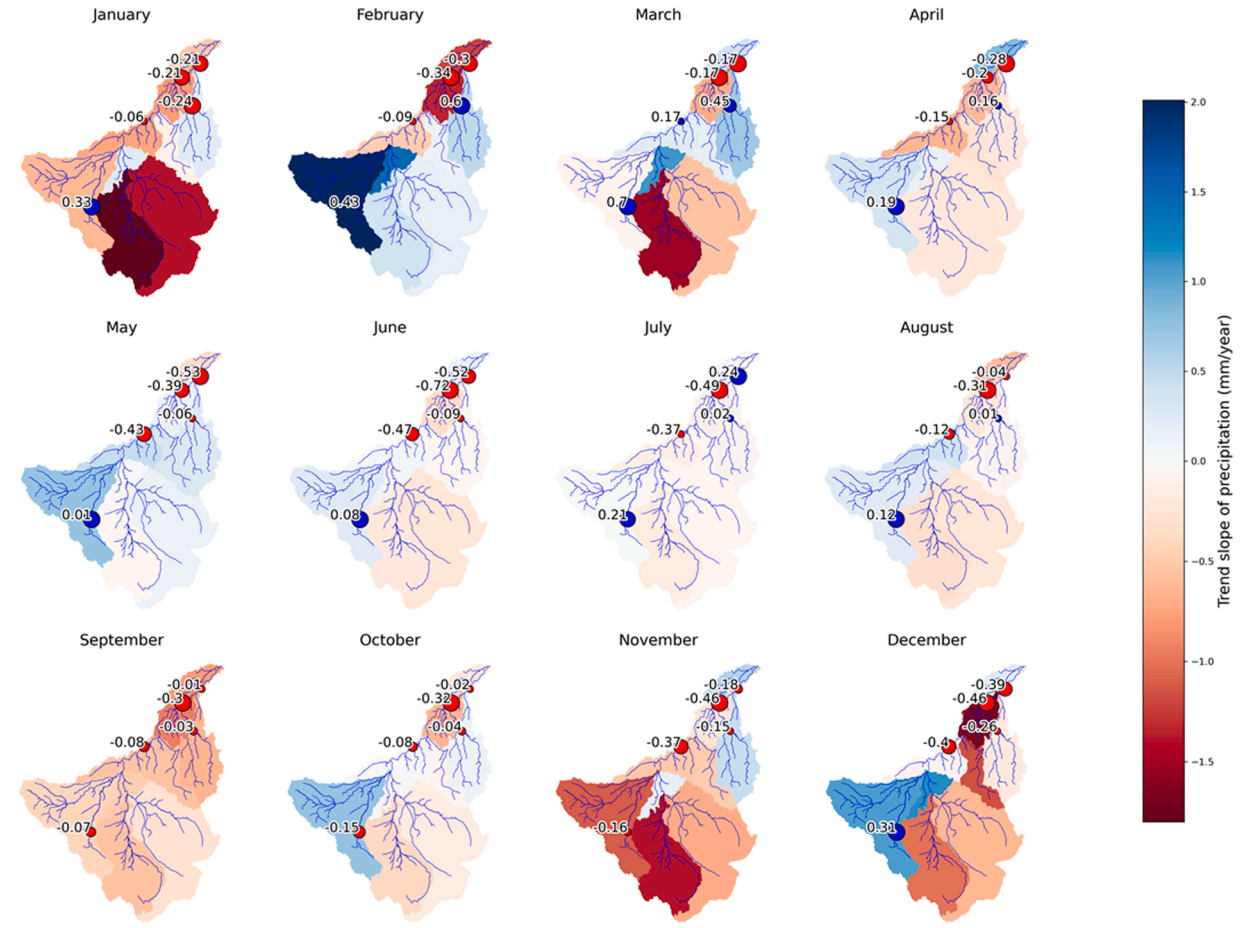

Fig. 9. Monthly trends (mm/ year) of precipitation and discharge across the nine subbasin of the Madeira River basin. The color scale represents the trend slope of precipitation, while the size of the points reflects the trend slope of discharge. Negative discharge trends are shown in red, and positive trends in blue.

offers useful information for studying the possible effects of deforestation on the basin hydrology. Reduced forest cover can initially increase surface runoff but may eventually reduce dry-season flows due to slowed water cycling and decreased groundwater recharge (Tomasella et al., 2008; von Randow et al., 2012). These changes highlight the complex dynamics between forest-atmosphere interactions, land-use changes, and climate in the Madeira River Basin.

4. Discussion

Our results on the analysis of forest cover changes in the Madeira River basin aligns with those of Souza et al. (2020), who investigated land use and land cover (LULC) changes across various biomes in Brazil from 1987 to 2017. They found that the Amazon biome, which comprises 49 % of the country, lost more forest area than any other biome due to the expansion of pasture. However, their analysis was limited to Brazil and did not include the Amazon regions in Bolivia and Peru. Lima et al. (2014) analysed deforestation patterns across the entire Amazon Basin from 2001 to 2021, demonstrating that the Madeira River basin has the lowest percentage of forest preservation in the Amazon, with only 54.6 % of forest cover remaining. Our results reinforce this significant forest degradation in the Madeira basin, while further detailing deforestation patterns at regional and subbasin scale.

The trend and change-point analysis of hydrological fluxes suggest an alteration in the regional hydrological cycle over the long-term analysis period (1981–2016). This alteration is characterized by more pronounced downward trends in annual evaporation and discharge compared to precipitation, particularly in the northern part of the basin. These findings align with previous research that has observed similar trends and hydrological changes in southern Amazonia. For instance, Heerspink et al. (2020) reported decreasing trends in rainfall and river flows, and Chagas et al. (2022) found substantial reductions in drought flows in this region despite minimal changes observed in climatic variables. Additionally, Lima et al. (2014), in their analysis of three basins in the southwestern Amazon (Jurua, Purus, and Madeira), also noted that the Madeira basin experienced a greater reduction in annual evaporation than in precipitation.

The seasonal and monthly trend analysis reveals significant increasing trends in precipitation and evaporation during the wet

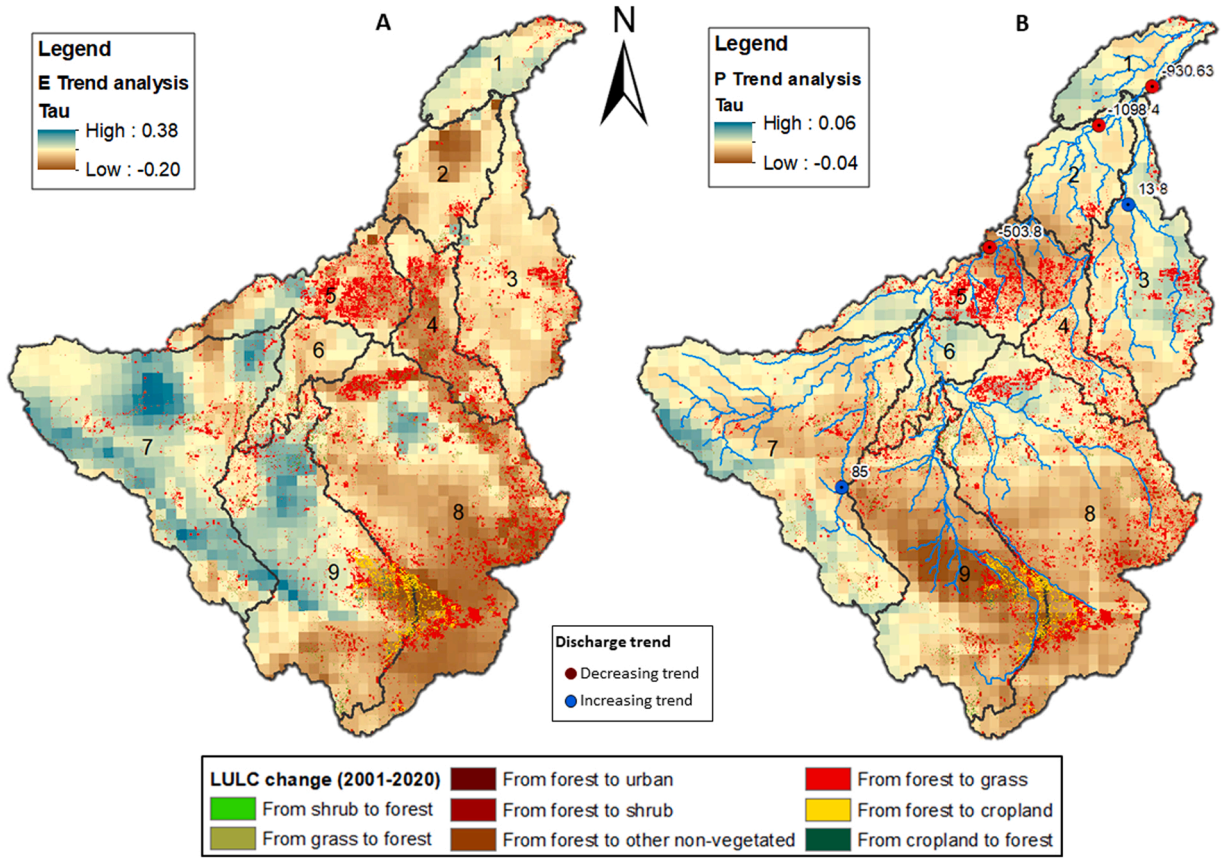

Fig. 10. Spatially-distributed analysis of variations in hydrological fluxes and forest coverage across the Madeira River basin. A. Tau value of the Mann-Kendall trend test for evaporation over the period along with loss of forest areas. B. Tau value of the Mann-Kendall trend test for precipitation, also shown with forest loss over the same period.

Table 3
Correlation between annual evaporation and forest area in the Madeira River subbasins. The table displays Spearman's rank correlation coefficients along with their respective p-values for annual evaporation and forest area (left) and the Spearman correlation between changes in evaporation and changes in forest (right). Statistically significant correlations ($p < 0.1$) are highlighted in bold.

Subbasin	Annual correlation	P value	Correlation between changes	P value
1	0.06	0.83	0.10	0.71
2	0.10	0.73	0.34	0.22
3	**0.50**	**0.06**	0.38	0.17
4	0.42	0.12	**0.47**	**0.08**
5	**0.46**	**0.08**	0.18	0.52
6	**−0.63**	**0.01**	−0.17	0.55
7	−0.01	0.98	−0.16	0.57
8	−0.09	0.74	**0.55**	**0.03**
9	0.36	0.18	**0.64**	**0.01**

season in the southwestern portion of the basin (subbasins 6 and 7). Segura et al. (2020) attribute the increase of precipitation to two atmospheric mechanisms. First, the Bolivian High (BH), an upper-level anticyclonic circulation system formed by intense surface heating in the Andean regions of Bolivia and Peru. The BH generates convective clouds that contribute to heavy rainfall from December to March and plays a critical role in modulating atmospheric circulation and precipitation patterns in the basin (Nobre et al., 2021; Rozante et al., 2022; Segura et al., 2019). Second, the upward motion over the western Amazon, a key component of the meridional circulation between the tropical North Atlantic and western South America, has intensified over the past two decades. This strengthening is associated with increased meridional moisture transport from the tropical North Atlantic, which leads to increased convection, and reduced atmospheric stability, ultimately contributing to higher precipitation. In contrast, the lower Madeira basin (subbasin 2), downstream of the most deforested areas, shows significant downward precipitation trends during the wet season. These findings align with those of Haghtalab et al. (2020) and (Silva Junior et al., 2018), who observed reduced annual precipitation, and an

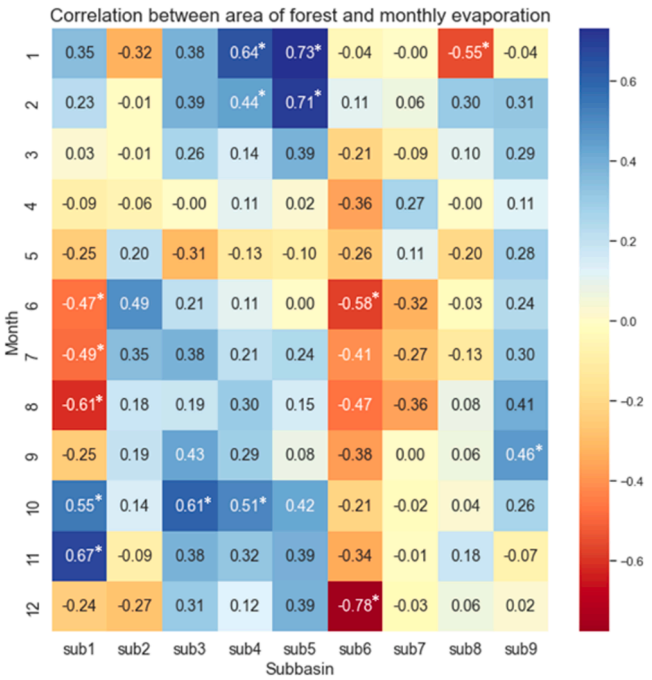

Fig. 11. Correlation coefficients between area of forest and monthly evaporation for the period of 2001–2015 per subbasin (numbers marked with an asterisk (*) indicate significance at the 10 % level).

Table 4
Correlation between annual discharge and forest area at three streamflow stations in the Madeira River basin. The table presents Spearman's rank correlation coefficients with corresponding p-values for annual discharge and forest area (left), and the correlation between changes in discharge and changes in forest area (right). Statistically significant correlations ($p < 0.1$) are highlighted in bold.

Name	Annual correlation	P value	Correlation between changes	P value
Porto Velho	**−0.46**	0.08	**0.48**	0.08
Manicore	−0.21	0.46	0.34	0.23
Fazenda	−0.18	0.52	0.41	0.13

increase in the number of dry days around Porto Velho, suggesting that the shift in wet/dry patterns may be linked to the expansion of grasslands in the region.

The strong positive correlation between forest cover and evaporation in January and February in the most deforested subbasins ($r = 0.73$, $p < 0.1$) may suggest a direct influence of forest cover on evaporation. The reduction in surface evaporation due to deforestation decreases atmospheric moisture availability for recycling, potentially suppressing convective feedback processes and affecting downstream precipitation (Coe et al., 2009; Flores et al., 2024; Nobre et al., 2021). Previous studies have demonstrated that transpiration from the rainforest significantly contributes to water vapor levels and precipitation during the onset of the monsoon season. Therefore, the transition from the dry to wet season in the southern Amazon is influenced by the amount of moisture released into the atmosphere through evapotranspiration from the Amazonian forest canopy (Nobre et al., 2021; Wright et al., 2017).

By finding significant correlations between forest cover and evaporation, as well as between the changes in forest cover and changes in evaporation, our study emphasizes the critical role of tropical forests in modulating the regional water cycle, particularly in the southern Amazon, supporting the results of previous studies (de Souza et al., 2022a; Lima et al., 2014; Siqueira et al., 2015; Tomasella et al., 2008; von Randow et al., 2012). According to the Science Panel for the Amazon (Nobre et al., 2021), approximately 28 % of atmospheric water vapor in the Amazon originates locally through forest evapotranspiration, while the remaining 72 % comes from oceanic sources. Although this estimate applies to the entire Amazon and not specifically to the Madeira basin, it suggests that part of the changes in evaporation processes may be linked to local deforestation, while another portion may be derived from broader climatic processes. Further research is required to determine the precise proportion of atmospheric vapor contributed by local forest processes in the Madeira basin, which could help disentangle the relative impacts of deforestation and climatic factors on regional hydrological dynamics.

In addition to changes in evaporation, the observed negative correlation between forest area and annual discharge at the Porto Velho station ($r = -0.46$ $p < 0.1$) combined with the positive correlation obtained between changes in forest and changes in discharge in the same station ($r = 0.48$ $p < 0.1$) suggests that in the highly impacted subbasins, such as 5 and 8, deforestation may have reduced

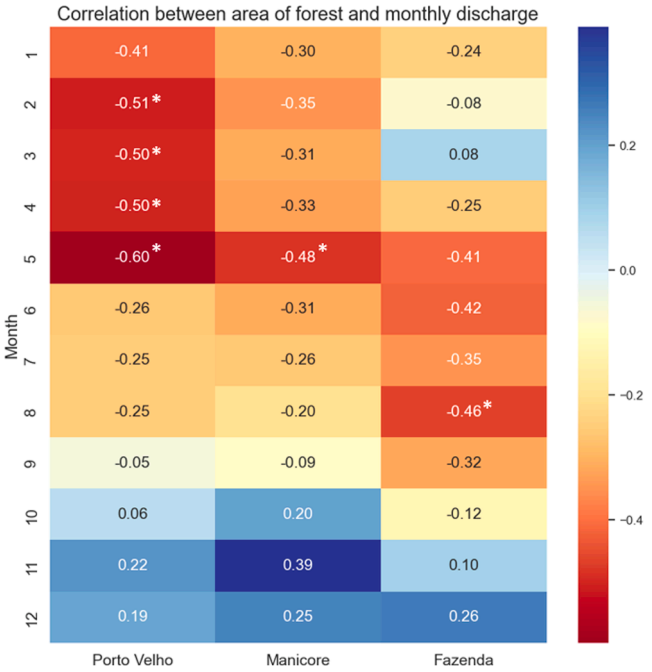

Fig. 12. Correlation coefficients between forest coverage and monthly discharge per station, including the p-value (The stations are organized from their location from upstream to downstream). the numbers marked with an asterisk (*) indicate significance at the 10 % level.

infiltration and evapotranspiration, contributing to increased surface runoff and streamflow. Similar findings have been reported in other studies of the Amazon, where deforestation-induced alterations to evapotranspiration and soil moisture dynamics have led to changes in streamflow patterns (Coe et al., 2009; Silva Junior et al., 2018). The decreasing strength of this correlation downstream, as observed at the Manicore station ($r = -0.21$), could reflect the combined influences of the basin size, hydrological buffering, and spatial variations in land use and climate dynamics. This aligns with Lima et al. (2014), who noted that larger basin areas often reduce localized land use impacts due to the integration of diverse land cover and hydrological conditions.

The intra-annual variation in correlation between forest cover and discharge with stronger negative associations during wet months ($r = -0.6$ in May at Porto Velho) confirms the seasonality of deforestation impacts on discharge. This may be linked to reduced infiltration capacity and increased surface runoff during periods of high precipitation. Similar seasonal sensitivities have been observed in studies of hydrological fluxes in the Amazon, where the loss of forest cover exacerbates peak flows during wet periods (Nobre et al., 2021; Towner et al., 2020). Moreover, the significant downward trend in evaporation during the wet season in half of the Madeira Basin (subbasins 2, 3, 4, 5, and 8), combined with the significant positive observed correlation between forest and evaporation, and the significant negative correlation between forest and discharge in the most deforested zones also during wet months, suggest that reduced evapotranspiration from deforested areas can suppress water recycling and delay the return of moisture to the atmosphere. This disruption in land-atmosphere interactions may contribute to shifts in the hydrological regime, intensifying flood risks during the wet season while potentially reducing streamflow resilience during dry periods (Coe et al., 2009; Nobre et al., 2021).

The negative correlation between forest cover and streamflow in the shorter period observed in Porto Velho station may reflects immediate deforestation impacts, such as reduced evapotranspiration and increased runoff, intensifying streamflow during wet months. In contrast, the long-term decreasing discharge trends observed at the same station and downstream stations may indicate broader climatic influences and weakened water recycling due to deforestation. This difference suggests that deforestation has both short-term effects, increasing flow, and long-term consequences, potentially slowing the water cycle through reduced precipitation and atmospheric moisture. Furthermore, extreme events, such as the 2014 severe flood may have had a stronger influence on the correlation observed in the shorter period (2001–2015) than on the longer period trends (1981–2016). This, highlights the potential for anomalous years to amplify correlations in short-term analysis, whereas the longer period trends may be more indicative of gradual shifts in the hydrological cycle.

These findings align with studies that link deforestation to alterations in the hydrological cycle, particularly through reduced evapotranspiration and its influence on precipitation patterns (Heerspink et al., 2020; Marengo et al., 2018; Siqueira et al., 2015). While some research suggests that deforestation increases river flow in certain regions (Cavalcante et al., 2019; Levy et al., 2018; Lima et al., 2014). Our results support the perspective that long-term reductions in evaporation contribute to broader shifts in precipitation and discharge trends, which aligns with Posada-Marín and Salazar (2022), who emphasized that reduced evaporation due to deforestation can suppress rainfall over large areas, ultimately leading to decreased river flow.

5. Conclusion

This study investigates the spatial and temporal changes in hydrological fluxes and their relationship with deforestation patterns in the Madeira River basin. Our results indicate a deforestation rate of 2810 km^2 per year from 2001 to 2020, with the highest percentage of deforestation observed in the Brazilian portion of the basin, primarily due to land conversion from forest to grass. The spatial and temporal analysis reveals a decreasing trend in precipitation, evaporation, and discharge from 1981 to 2016, with the strongest negative trends observed for evaporation during the wet season and in the most deforested regions. The annual correlation analysis reveals significant positive relationships between forest area and evaporation ($r = 0.5$) and between changes in forest area and changes in evaporation ($r = 0.47$). These correlations are most pronounced in the middle basin, where deforestation is most extensive. Additionally, monthly correlation analysis indicates that evaporation is more sensitive to forest cover during the wet season, with the highest positive correlation observed in this period ($r = 0.73$).

Moreover, the analysis reveals significant negative correlations between forest cover and discharge ($r = -0.46$), and significant positive correlation between changes in forest cover and changes in discharge ($r = -0.48$) in the central part of the southern basin where deforestation is higher. These findings support the hypothesis that large-scale deforestation reduces evapotranspiration, disrupts the precipitation-evaporation feedback and may intensify wet season streamflow mainly as a result of increased surface runoff. However, the observed decreasing trends in streamflow over the long term may suggest a gradual weakening of the water cycle, potentially driven by broader climatic changes and a reduction in regional moisture recycling. The deforestation over the period has significantly affected the streamflow regime in the basin, particularly during the dry season as evidenced in the Manicore station, where the monthly average discharge in October decreased by approximately 34 % when comparing the post-change point period (1996–2016) with the pre-change point period (1981–1995).

The results of this study highlight the potential of deforestation in altering the hydrological cycle within the Madeira basin. Forests play a critical role in sustaining evapotranspiration, infiltration, and precipitation feedback processes, which collectively regulate streamflow dynamics. However, several limitations of the study should be acknowledged. First, the analysis was constrained by the availability of land use change and streamflow data, limiting the temporal scope of the correlation analysis between the forest cover and hydrological variables to 2001–2015. This timeframe may not fully capture long-term trends or the cumulative impacts of deforestation over decades. Second, the attribution of observed trends to deforestation versus broader climatic drivers remains challenging, considering that changes in precipitation patterns, atmospheric dynamics, and extreme weather events all play interconnected roles. In particular, the absence of controls for large-scale climate phenomena such as the El Niño–Southern Oscillation (ENSO) and the Pacific Decadal Oscillation (PDO) may confound or interact with land-use effects, making causal attribution difficult. Additionally, uncertainties remain regarding the interactions with other variables such as groundwater and the impact of additional drivers such as non-stationary climate. Thus, the next stage of this research will include a process-based (mechanistic) hydrological modelling analysis incorporating recently released streamflow data and higher-resolution hydroclimatic datasets to complement the current study and improve the understanding of the impact of deforestation on hydrological processes in the Madeira basin.

CRediT authorship contribution statement

Dimitri Solomatine: Writing – review & editing. **Remko Uijlenhoet:** Writing – review & editing, Conceptualization. **Gerald Corzo:** Writing – review & editing, Conceptualization. **Shreedhar Maskey:** Writing – review & editing, Supervision, Methodology, Conceptualization. **Eliana Torres:** Writing – original draft, Methodology, Investigation, Funding acquisition, Formal analysis, Conceptualization.

Declaration of Competing Interest

The authors declare that they have no known competing financial interests or personal relationships that could have appeared to influence the work reported in this paper.

Acknowledgements

This study was financially supported by the Mexican National Council for Science and Technology (CONACYT) with the study grand 2021–000014–01EXTF-00099 and the Colombian Ministry of Science, Tecnology and Innovation (Minciencias), with the Scholarship Program No. 906.

Appendix A. Supporting information

Supplementary data associated with this article can be found in the online version at doi:10.1016/j.ejrh.2025.102680.

Data Availability

All datasets used in this study are publicly available from the following sources:•

CHIRPS v2.0 Precipitation dataset: https://www.chc.ucsb.edu/data/chirps•

GLEAM v3.8a Evaporation dataset: https://www.gleam.eu•

MODIS MCD12Q1 Version 6.1 Land Cover product: provided by NASA LP DAAC – https://lpdaac.usgs.gov/products/mcd12q1v061/•

Streamflow data (Brazil): obtained from the CAMELS-BR dataset (version 1.1) (Chagas et al., 2020), available at: https://zenodo.org/records/15025488•

Brazilian hydrometric data: also available from the National Water and Sanitation Agency (ANA) platform: https://www.snirh.gov.br/hidroweb•

Streamflow data (Bolivia): obtained from the SO HYBAM Observatory: https://hybam.obs-mip.fr

Additional figures are provided in the Supplementary Materials, and the Python code used for our analysis can be shared upon request for research purposes.

References

Abdulkareem, J.H., Pradhan, B., Sulaiman, W.N.A., Jamil, N.R., 2019. Long-term runoff dynamics assessment measured through land use/cover (LULC) changes in a tropical complex catchment. Environ. Syst. Decis. 39 (1), 16–33. https://doi.org/10.1007/s10669-018-9696-3.

ANA), 2011. Qualificação de dados hidrológicos e reconstituição de vazões naturais no país. Brasília, Brazil. Agência Nacional de Águas.

Anderson, B.J., Slater, L.J., Dadson, S.J., Blum, A.G., Prosdocimi, I., 2022. Statistical attribution of the influence of urban and tree cover change on streamflow: a comparison of large sample statistical approaches. Water Resour. Res. 58 (5). https://doi.org/10.1029/2021WR030742.

Ayalew, S.E., Niguse, T.A., Aragaw, H.M., 2024. Hydrological responses to historical and predicted land use/land cover changes in the welmel watershed, genale dawa basin, Ethiopia: implications for water resource management. J. Hydrol. Reg. Stud. 52. https://doi.org/10.1016/j.ejrh.2024.101709.

Baker, J.C.A., Garcia-Carreras, L., Gloor, M., Marsham, J.H., Buermann, W., Da Rocha, H.R., Nobre, A.D., De Carioca Araujo, A., Spracklen, D.V., 2021. Evapotranspiration in the Amazon: spatial patterns, seasonality, and recent trends in observations, reanalysis, and climate models. Hydrol. Earth Syst. Sci. 25 (4), 2279–2300. https://doi.org/10.5194/hess-25-2279-2021.

Blum, A.G., Ferraro, P.J., Archfield, S.A., Ryberg, K.R., 2020. Causal effect of impervious cover on annual flood magnitude for the United States. Geophys. Res. Lett. 47 (5). https://doi.org/10.1029/2019GL086480.

Cavalcante, R.B.L., Pontes, P.R.M., Souza-Filho, P.W.M., de Souza, E.B., 2019. Opposite effects of climate and land use changes on the annual water balance in the Amazon arc of deforestation. Water Resour. Res. 55 (4), 3092–3106. https://doi.org/10.1029/2019WR025083.

Chagas, V.B.P., L. B. Chaffe, P., Addor, N., M. Fan, F., S. Fleischmann, A., C. D. Paiva, R., Siqueira, V.A., 2020. CAMELS-BR: hydrometeorological time series and landscape attributes for 897 catchments in Brazil. Earth Syst. Sci. Data 12 (3), 2075–2096. https://doi.org/10.5194/essd-12-2075-2020.

Chagas, V.B.P., Chaffe, P.L.B., Blöschl, G., 2022. Climate and land management accelerate the Brazilian water cycle. Nat. Commun. 13 (1). https://doi.org/10.1038/s41467-022-32580-x.

Coe, M.T., Costa, M.H., Soares-Filho, B.S., 2009. The influence of historical and potential future deforestation on the stream flow of the Amazon River - land surface processes and atmospheric feedbacks. J. Hydrol. 369 (1–2), 165–174. https://doi.org/10.1016/j.jhydrol.2009.02.043.

Conte, L.C., Bayer, D.M., Bayer, F.M., 2019. Bootstrap pettitt test for detecting change points in hydroclimatological data: case study of itaipu hydroelectric plant, Brazil. Hydrol. Sci. J. 64 (11), 1312–1326. https://doi.org/10.1080/02626667.2019.1632461.

De Souza, V.A.S., Moreira, D.M., Filho, O.C.R., Rudke, A.P., Andrade, C.D., De Araujo, L.M.N., 2022b. Spatio-temporal analysis of remotely sensed rainfall datasets retrieved for the transboundary basin of the Madeira river in amazonia. Atmosfera 35 (1), 39–66. https://doi.org/10.20937/ATM.52783.

Dias, L.C.P., Macedo, M.N., Costa, M.H., Coe, M.T., Neill, C., 2015. Effects of land cover change on evapotranspiration and streamflow of small catchments in the upper Xingu river basin, central Brazil. J. Hydrol. Reg. Stud. 4 (PB), 108–122. https://doi.org/10.1016/j.ejrh.2015.05.010.

Eltahir, E.A.B., 1996. Role of vegetation in sustaining large-scale atmospheric circulations in the tropics. J. Geophys. Res. Atmospheres 101 (D2), 4255–4268. https://doi.org/10.1029/95JD03632.

Espinoza Villar, J.C., Guyot, J.L., Ronchail, J., Cochonneau, G., Filizola, N., Fraizy, P., Labat, D., de Oliveira, E., Ordoñez, J.J., Vauchel, P., 2009. Contrasting regional discharge evolutions in the Amazon basin (1974-2004). J. Hydrol. 375 (3–4). https://doi.org/10.1016/j.jhydrol.2009.03.004.

Estoque, R.C., Dasgupta, R., Winkler, K., Avitabile, V., Johnson, B.A., Myint, S.W., Gao, Y., Ooba, M., Murayama, Y., Lasco, R.D., 2022. Spatiotemporal pattern of global forest change over the past 60 years and the forest transition theory. Environ. Res. Lett. 17 (8). https://doi.org/10.1088/1748-9326/ac7df5.

Fassoni-Andrade, A.C., Fleischmann, A.S., Papa, F., Paiva, R.C.D. de, Wongchuig, S., Melack, J.M., Moreira, A.A., Paris, A., Ruhoff, A., Barbosa, C., Maciel, D.A., Novo, E., Durand, F., Frappart, F., Aires, F., Abrahão, G.M., Ferreira-Ferreira, J., Espinoza, J.C., Laipelt, L., … Pellet, V. (2021). Amazon Hydrology From Space: Scientific Advances and Future Challenges. In *Reviews of Geophysics* (Vol. 59, Issue 4). John Wiley and Sons Inc. https://doi.org/10.1029/2020RG000728.

Ferreira, L.A., Floreano, I.X., 2022. LULC zoning in the "Madeira river" settlement, legal Amazon, Brazil, before and after implementation of the rural environmental registry (CAR) (2008-2018). Environ. Dev. 43. https://doi.org/10.1016/j.envdev.2022.100725.

Flores, B.M., Montoya, E., Sakschewski, B., Nascimento, N., Staal, A., Betts, R.A., Levis, C., Lapola, D.M., Esquível-Muelbert, A., Jakovac, C., Nobre, C.A., Oliveira, R. S., Borma, L.S., Nian, D., Boers, N., Hecht, S.B., ter Steege, H., Arieira, J., Lucas, I.L., Hirota, M., 2024. Critical transitions in the Amazon forest system. Nature 626 (7999), 555–564. https://doi.org/10.1038/s41586-023-06970-0.

Friedl, M., & Sulla-Menashe, D. (2022). MODIS/Terra+Aqua Land Cover Type Yearly L3 Global 500m SIN Grid V061 [Data set]. *NASA EOSDIS Land Processes Distributed Active Archive Center*.

Funk, C., Peterson, P., Landsfeld, M., Pedreros, D., Verdin, J., Shukla, S., Husak, G., Rowland, J., Harrison, L., Hoell, A., Michaelsen, J., 2015. The climate hazards infrared precipitation with stations - a new environmental record for monitoring extremes. Sci. Data 2. https://doi.org/10.1038/sdata.2015.66.

Gomes, W. de B., Satyamurty, P., Correia, F.W.S., Chou, S.C., Vergasta, L.A., de Arruda Lyra, A., 2022. Intraseasonal scale ensemble forecasts of precipitation and evapotranspiration for the Madeira river basin using different physical parameterizations. Atmos. Res. 270. https://doi.org/10.1016/j.atmosres.2022.106086.

Gotlieb, Y., García Girón, J.D., 2020. The role of land use conversion in shaping the land cover of the central American dry corridor. Land Use Policy 94. https://doi.org/10.1016/j.landusepol.2019.104351.

Gutierrez-Cori, O., Espinoza, J.C., Li, L.Z.X., Wongchuig, S., Arias, P.A., Ronchail, J., Segura, H., 2021. On the Hydroclimate-Vegetation relationship in the southwestern Amazon during the 2000–2019 period. Front. Water 3. https://doi.org/10.3389/frwa.2021.648499.

Guzha, A.C., Rufino, M.C., Okoth, S., Jacobs, S., Nóbrega, R.L.B., 2018. Impacts of land use and land cover change on surface runoff, discharge and low flows: evidence from east Africa. J. Hydrol. Reg. Stud. 15, 49–67. https://doi.org/10.1016/j.ejrh.2017.11.005.

Haghtalab, N., Moore, N., Heerspink, B.P., Hyndman, D.W., 2020. Evaluating spatial patterns in precipitation trends across the Amazon basin driven by land cover and global scale forcings. Theor. Appl. Climatol. 140 (1–2), 411–427. https://doi.org/10.1007/s00704-019-03085-3.

Heerspink, B.P., Kendall, A.D., Coe, M.T., Hyndman, D.W., 2020. Trends in streamflow, evapotranspiration, and groundwater storage across the Amazon basin linked to changing precipitation and land cover. J. Hydrol. Reg. Stud. 32. https://doi.org/10.1016/j.ejrh.2020.100755.

Helsel, D.R., Hirsch, R.M., 2002. Chapter A3 - statistical methods in water resources, book 4 - hydrologic analysis and interpretation. Tech. Water Resour. Investig. U. S. Geol. Surv.

Helsel, D.R., Hirsch, R.M., Ryberg, K.R., Archfield, S.A., and Gilroy, E.J., 2020, Statistical methods in water resources: U.S. Geological Survey Techniques and Methods, book 4, chap. A3, 458 p., https://doi.org/10.3133/tm4a3. [Supersedes USGS Techniques of Water-Resources Investigations, book 4, chap. A3, version 1.1.].

Horton, A.J., Nygren, A., Diaz-Perera, M.A., Kummu, M., 2021. Flood severity along the usumacinta river, Mexico: identifying the anthropogenic signature of tropical forest conversion. J. Hydrol. X 10. https://doi.org/10.1016/j.hydroa.2020.100072.

Hu, Y., Maskey, S., Uhlenbrook, S., 2012. Trends in temperature and rainfall extremes in the Yellow River source region, China. Clim. Change 110 (1–2), 403–429. https://doi.org/10.1007/s10584-011-0056-2.

Hung, C.L.J., James, L.A., Carbone, G.J., Williams, J.M., 2020. Impacts of combined land-use and climate change on streamflow in two nested catchments in the southeastern United States. Ecol. Eng. 143. https://doi.org/10.1016/j.ecoleng.2019.105665.

Kendall, M.G., 1975. Rank Correlation Methods, 4th edn. Charles Griffin, *San Francisco, CA*.

Laureanti, N.C., Tavares, P. da S., Tavares, M., Rodrigues, D.C., Gomes, J.L., Chou, S.C., Correia, F.W.S., 2024. Extreme seasonal droughts and floods in the Madeira river basin, Brazil: diagnosis, causes, and trends. Climate 12 (8). https://doi.org/10.3390/cli12080111.

Lehner, B. (2014). *HydroBASINS Global watershed boundaries and sub-basin delineations derived from HydroSHEDS data at 15 s resolution Technical Documentation Version 1.c (with and without inserted lakes) prepared by.* ⟨http://www.hydrosheds.org⟩.

Levy, M.C., Lopes, A.V., Cohn, A., Larsen, L.G., Thompson, S.E., 2018. Land use change increases streamflow across the arc of deforestation in Brazil. Geophys. Res. Lett. 45 (8), 3520–3530. https://doi.org/10.1002/2017GL076526.

Lima, L.S., Coe, M.T., Soares Filho, B.S., Cuadra, S.V., Dias, L.C.P., Costa, M.H., Lima, L.S., Rodrigues, H.O., 2014. Feedbacks between deforestation, climate, and hydrology in the southwestern Amazon: implications for the provision of ecosystem services. Landsc. Ecol. 29 (2), 261–274. https://doi.org/10.1007/s10980-013-9962-1.

Mann, H.B., 1945. Mann nonparametric test against trend. Econometrica 13.

Marengo, J.A., 2005. Characteristics and spatio-temporal variability of the Amazon River basin water budget. Clim. Dyn. 24 (1), 11–22. https://doi.org/10.1007/s00382-004-0461-6.

Marengo, J.A., Souza, C.M., Thonicke, K., Burton, C., Halladay, K., Betts, R.A., Alves, L.M., Soares, W.R., 2018. Changes in climate and land use over the Amazon region: current and future variability and trends. In: Frontiers in Earth Science, 6. Frontiers Media S.A. https://doi.org/10.3389/feart.2018.00228.

Martens, B., Miralles, D.G., Lievens, H., Van Der Schalie, R., De Jeu, R.A.M., Fernández-Prieto, D., Beck, H.E., Dorigo, W.A., Verhoest, N.E.C., 2017. GLEAM v3: Satellite-based land evaporation and root-zone soil moisture. Geosci. Model Dev. 10 (5). https://doi.org/10.5194/gmd-10-1903-2017.

Min, T. (2006). Assessment of the effects of climate variability and land use change on the hydrology of the meuse river basin [Institute for Water Education te Delft]. In Atlantic. http://dare.ubvu.vu.nl/bitstream/1871/10234/1/Tu_Min_PhD_Thesis.pdf.

Miralles, D.G., Holmes, T.R.H., De Jeu, R.A.M., Gash, J.H., Meesters, A.G.C.A., Dolman, A.J., 2011. Global land-surface evaporation estimated from satellite-based observations. Hydrol. Earth Syst. Sci. 15 (2), 453–469. https://doi.org/10.5194/hess-15-453-2011.

Miralles, D.G., Jiménez, C., Jung, M., Michel, D., Ershadi, A., Mccabe, M.F., Hirschi, M., Martens, B., Dolman, A.J., Fisher, J.B., Mu, Q., Seneviratne, S.I., Wood, E.F., Fernández-Prieto, D., 2016. The WACMOS-ET project - part 2: evaluation of global terrestrial evaporation data sets. Hydrol. Earth Syst. Sci. 20 (2), 823–842. https://doi.org/10.5194/hess-20-823-2016.

Molina-Carpio, J., Espinoza, J.C., Vauchel, P., Ronchail, J., Gutierrez Caloir, B., Guyot, J.L., Noriega, L., 2017. Hydroclimatology of the upper Madeira river basin: spatio-temporal variability and trends. Hydrol. Sci. J. 62 (6), 911–927. https://doi.org/10.1080/02626667.2016.1267861.

Müller, R., Pacheco, P., & Montero, J.C. (2014). The context of deforestation and forest degradation in Bolivia. In *Bogor, Indonesia: Center for …*.

Nguyen, Q., Kantoush, S.A., Tran, T.N.D., Van Binh, D., Vo, N.D., Saber, M., Sumi, T., 2023. Response of hydrological to anthropogenic activities in a tropical basin binh. Proc. IAHR World Congr. https://doi.org/10.3850/978-90-833476-1-5_iahr40wc-p1339-cd.

Nobre, C., Encalada, A., Anderson, E., Roca Alcazar, F.H., Bustamante, M., Mena, C., Peña-Claros, M., Poveda, G., Rodriguez, J.P., Saleska, S., Trumbore, S.E., Val, A., Villa Nova, L., Abramovay, R., Alencar, A., Rodriguez Alzza, A.C., Armenteras, D., Artaxo, P., Athayde, S., Zapata-Ríos, G. (Eds.), 2021. Amazon Assessment Report 2021. UN Sustainable Development Solutions Network (SDSN). https://doi.org/10.55161/RWSX6527.

Oudin, L., Salavati, B., Furusho-Percot, C., Ribstein, P., Saadi, M., 2018. Hydrological impacts of urbanization at the catchment scale. J. Hydrol. 559, 774–786. https://doi.org/10.1016/j.jhydrol.2018.02.064.

Paca, V.H., da, M., Espinoza-Dávalos, G.E., Hessels, T.M., Moreira, D.M., Comair, G.F., Bastiaanssen, W.G.M., 2019. The spatial variability of actual evapotranspiration across the Amazon River basin based on remote sensing products validated with flux towers. Ecol. Process. 8 (1). https://doi.org/10.1186/s13717-019-0158-8.

Paca, V.H., da, M., Espinoza-Dávalos, G.E., Moreira, D.M., Comair, G., 2020. Variability of trends in precipitation across the Amazon River basin determined from the CHIRPS precipitation product and from station records. Water (Switz.) 12 (5). https://doi.org/10.3390/W12051244.

Paiva, K., Rau, P., Montesinos, C., Lavado-Casimiro, W., Bourrel, L., Frappart, F., 2023. Hydrological response assessment of land cover change in a Peruvian amazonian basin impacted by deforestation using the SWAT model. Remote Sens. 15 (24). https://doi.org/10.3390/rs15245774.

Papastefanou, P., Zang, C.S., Angelov, Z., De Castro, A.A., Jimenez, J.C., De Rezende, L.F.C., Ruscica, R.C., Sakschewski, B., Sörensson, A.A., Thonicke, K., Vera, C., Viovy, N., Von Randow, C., Rammig, A., 2022. Recent extreme drought events in the Amazon rainforest: assessment of different precipitation and evapotranspiration datasets and drought indicators. Biogeosciences 19 (16), 3843–3861. https://doi.org/10.5194/bg-19-3843-2022.

Paredes-Trejo, F., Barbosa, H.A., Giovannettone, J., Lakshmi Kumar, T.V., Thakur, M.K., De Oliveira Buriti, C., 2021. Long-term spatiotemporal variation of droughts in the Amazon River basin. Water (Switz.) 13 (3). https://doi.org/10.3390/w13030351.

Pettitt, A.N., 1979. A non-parametric approach to the change-point problem. Appl. Stat. 28 (2). https://doi.org/10.2307/2346729.

Posada-Marín, J.A., Salazar, J.F., 2022. River flow response to deforestation: contrasting results from different models. In: Water Security, 15. Elsevier B.V. https://doi.org/10.1016/j.wasec.2022.100115.

Rogger, M., Agnoletti, M., Alaoui, A., Bathurst, J.C., Bodner, G., Borga, M., Chaplot, V., Gallart, F., Glatzel, G., Hall, J., Holden, J., Holko, L., Horn, R., Kiss, A., Kohnová, S., Leitinger, G., Lennartz, B., Parajka, J., Perdigão, R., Blöschl, G., 2017. Land use change impacts on floods at the catchment scale: challenges and opportunities for future research. In: Water Resources Research, 53. Blackwell Publishing Ltd, pp. 5209–5219. https://doi.org/10.1002/2017WR020723.

Rozante, J.R., Ramirez, E., Fernandes, A. de A., 2022. A newly developed south American mapping of temperature with estimated lapse rate corrections. Int. J. Climatol. 42 (4), 2135–2152. https://doi.org/10.1002/joc.7356.

Saraiva Okello, A.M.L., Masih, I., Uhlenbrook, S., Jewitt, G.P.W., Van Der Zaag, P., Riddell, E., 2015. Drivers of spatial and temporal variability of streamflow in the incomati river basin. Hydrol. Earth Syst. Sci. 19 (2), 657–673. https://doi.org/10.5194/hess-19-657-2015.

Segura, H., Junquas, C., Espinoza, J.C., Vuille, M., Jauregui, Y.R., Rabatel, A., Condom, T., Lebel, T., 2019. New insights into the rainfall variability in the tropical Andes on seasonal and interannual time scales. Clim. Dyn. 53 (1–2), 405–426. https://doi.org/10.1007/s00382-018-4590-8.

Segura, H., Espinoza, J.C., Junquas, C., Lebel, T., Vuille, M., Garreaud, R., 2020. Recent changes in the precipitation-driving processes over the Southern tropical Andes/Western Amazon. Clim. Dyn. 54 (5–6), 2613–2631. https://doi.org/10.1007/s00382-020-05132-6.

Sen, P.K., 1968. Estimates of the regression coefficient based on Kendall's tau. J. Am. Stat. Assoc. 63 (324). https://doi.org/10.1080/01621459.1968.10480934.

Sikora de Souza, V.A., Moreira, D.M., Rotunno Filho, O.C., Rudke, A.P., 2020. Extreme rainfall events in amazonia: the Madeira river basin. Remote Sens. Appl. Soc. Environ. 18. https://doi.org/10.1016/j.rsase.2020.100316.

da Silva Cruz, J., Blanco, C.J.C., de Oliveira Júnior, J.F., 2022. Modeling of land use and land cover change dynamics for future projection of the Amazon number curve. Sci. Total Environ. 811. https://doi.org/10.1016/j.scitotenv.2021.152348.

Silva Junior, C.H.L., Almeida, C.T., Santos, J.R.N., Anderson, L.O., Aragão, L.E.O.C., Silva, F.B., 2018. Spatiotemporal rainfall trends in the Brazilian legal Amazon between the years 1998 and 2015. Water (Switz.) 10 (9). https://doi.org/10.3390/w10091220.

Siqueira, J.L., Tomasella, J., Rodriguez, D.A., 2015. Impacts of future climatic and land cover changes on the hydrological regime of the Madeira river basin. Clim. Change 129 (1–2), 117–129. https://doi.org/10.1007/s10584-015-1338-x.

Slater, L., Villarini, G., Archfield, S., Faulkner, D., Lamb, R., Khouakhi, A., Yin, J., 2021. Global changes in 20-Year, 50-Year, and 100-Year river floods. Geophys. Res. Lett. 48 (6). https://doi.org/10.1029/2020GL091824.

Souza, C.M., Shimbo, J.Z., Rosa, M.R., Parente, L.L., Alencar, A.A., Rudorff, B.F.T., Hasenack, H., Matsumoto, M., Ferreira, L.G., Souza-Filho, P.W.M., de Oliveira, S. W., Rocha, W.F., Fonseca, A.V., Marques, C.B., Diniz, C.G., Costa, D., Monteiro, D., Rosa, E.R., Vélez-Martin, E., Azevedo, T., 2020. Reconstructing three decades of land use and land cover changes in Brazilian biomes with landsat archive and earth engine. Remote Sens. 12 (17). https://doi.org/10.3390/RS12172735.

de Souza, V.A.S., Filho, O.C.R., Rodriguez, D.A., Moreira, D.M., Rudke, A.P., Andrade, C.D., 2022a. Dynamics of forest conversion and climate trends in the Madeira river basin. Cienc. Florest. 32 (4), 2007–2034. https://doi.org/10.5902/1980509865211.

Staal, A., Flores, B.M., Aguiar, A.P.D., Bosmans, J.H.C., Fetzer, I., Tuinenburg, O.A., 2020. Feedback between drought and deforestation in the Amazon. Environ. Res. Lett. 15 (4). https://doi.org/10.1088/1748-9326/ab738e.

Stickler, C.M., Coe, M.T., Costa, M.H., Nepstad, D.C., McGrath, D.G., Dias, L.C.P., Rodrigues, H.O., Soares-Filho, B.S., 2013. Dependence of hydropower energy generation on forests in the Amazon basin at local and regional scales. Proc. Natl. Acad. Sci. USA 110 (23), 9601–9606. https://doi.org/10.1073/pnas.1215331110.

Theil, H. (1950). A rank-invariant method of linear and polynomial regression analysis, Part I. In *Proceedings of the Royal Netherlands Academy of Sciences: Vol. LIII*.

Tomasella, J., Hodnett, M.G., Cuartas, L.A., Nobre, A.D., Waterloo, M.J., Oliveira, S.M., 2008. The water balance of an amazonian micro-catchment: the effect of interannual variability of rainfall on hydrological behaviour. Hydrol. Process. 22 (13), 2133–2147. https://doi.org/10.1002/hyp.6813.

Towner, J., Cloke, H.L., Lavado, W., Santini, W., Bazo, J., Coughlan de Perez, E., Stephens, E.M., 2020. Attribution of Amazon floods to modes of climate variability: a review. Meteorol. Appl. 27 (5). https://doi.org/10.1002/met.1949.

Trancoso, R., Carneiro Filho, A., Tomasella, J., Schietti, J., Forsberg, B.R., Miller, R.P., 2009. Deforestation and conservation in major watersheds of the Brazilian Amazon. Environ. Conserv. 36 (4), 277–288. https://doi.org/10.1017/S0376892909990373.

Tsiokanos, A., Rutten, M., Van Der Ent, R.J., Uijlenhoet, R., 2024. Flood drivers and trends: a case study of the geul river catchment (the Netherlands) over the past half century. Hydrol. Earth Syst. Sci. 28 (14), 3327–3345. https://doi.org/10.5194/hess-28-3327-2024.

Van Der Ent, R.J., Savenije, H.H.G., Schaefli, B., Steele-Dunne, S.C., 2010. Origin and fate of atmospheric moisture over continents. Water Resour. Res. 46 (9). https://doi.org/10.1029/2010WR009127.

Vergasta, L.A., Correia, F.W.S., Satyamurty, P., Chou, S.C., Lyra, A., de, A., Gomes, W., de, B., Fleischmann, A., Papa, F., 2023. An assessment of the present hydroclimatic regime of the Madeira river basin using climate and hydrological models. Hydrol. Sci. J. 68 (10), 1338–1357. https://doi.org/10.1080/02626667.2023.2216844.

von Randow, R.C.S., von Randow, C., Hutjes, R.W.A., Tomasella, J., Kruijt, B., 2012. Evapotranspiration of deforested areas in central and southwestern amazonia. Theor. Appl. Climatol. 109 (1–2), 205–220. https://doi.org/10.1007/s00704-011-0570-1.

Weng, W., Luedeke, M., Zemp, D., Lakes, T., Kropp, J., 2018. Aerial and surface rivers: downwind impacts on water availability from land use changes in amazonia. Hydrol. Earth Syst. Sci. 22 (1), 911–927. https://doi.org/10.5194/hess-22-911-2018.

Wright, J.S., Fu, R., Worden, J.R., Chakraborty, S., Clinton, N.E., Risi, C., Sun, Y., Yin, L., 2017. Rainforest-initiated wet season onset over the Southern Amazon. Proc. Natl. Acad. Sci. USA 114 (32), 8481–8486. https://doi.org/10.1073/pnas.1621516114.

Wu, F., Zhan, J., Su, H., Yan, H., Ma, E., 2015. Scenario-Based impact assessment of land Use/Cover and climate changes on watershed hydrology in heihe river basin of northwest China. Adv. Meteorol. 2015. https://doi.org/10.1155/2015/410198.

Yang, W., Yang, H., Yang, D., Hou, A., 2021. Causal effects of dams and land cover changes on flood changes in mainland China. Hydrol. Earth Syst. Sci. 25 (5). https://doi.org/10.5194/hess-25-2705-2021.

Yang, X., Chen, H., Wang, Y., Xu, C.Y., 2016. Evaluation of the effect of land use/cover change on flood characteristics using an integrated approach coupling land and flood analysis. Hydrol. Res. 47 (6), 1161–1171. https://doi.org/10.2166/nh.2016.108.

Yue, S., Pilon, P., Cavadias, G., 2002. Power of the Mann-Kendall and Spearman's rho tests for detecting monotonic trends in hydrological series. J. Hydrol. 259 (1–4). https://doi.org/10.1016/S0022-1694(01)00594-7.

Zemp, D.C., Schleussner, C.F., Barbosa, H.M.J., Van Der Ent, R.J., Donges, J.F., Heinke, J., Sampaio, G., Rammig, A., 2014. On the importance of cascading moisture recycling in South America. Atmos. Chem. Phys. 14 (23), 13337–13359. https://doi.org/10.5194/acp-14-13337-2014.